CHARACTERIZATION OF MERCURY TELLURIDE

Mojtaba Kahrizi

A Thesis

in

Department of Physics

Presented in Partial Fulfillment of the Requirements
for the degree of Master of Science at
Concordia University
Montréal, Québec, Canada

April 1980

©Mojtaba Kahrizi, 1980

ABSTRACT

CHARACTERIZATION OF MERCURY TELLURIDE

Mojtaba Kahrizi

Mercury telluride samples were grown by the Bridgeman technique. Electrical resistivity and Hall mobility as a function of temperature (from 4.2 K to 300 K) for a total of four samples were measured. The magnetic field dependence of the Hall coefficient was determined.

A value of 0.01 - 0.03 ev for the energy gap was obtained. By using the "Two Band Model" the two different carriers in the samples were characterized. The samples were n-type for the entire temperature range, and the p - to - n transition was not observed.

TABLE OF CONTENTS

LIST OF FIGURES

LIST OF TABLES

ACKNOWLEDGEMENTS

CHARACTERIZATION OF MERCURY TELLURIDE

Mojtaba Kahrizi

I wish to express my thanks to my research supervisor, Dr. J.A. Mackinnon, for his guidance and co-operation during the period of this work.

I would also like to thank Dr. B.A. Lombos for his unhesitated advices.

Nomenclature of References and Mathematical Equations

References in this thesis are given by reference number within parenthesis.

Mathematical equation are given by, Ch. No. ..Eq. No., within parenthesis, e.g. (2.3) means equation no. (3) of chapter (2) .

CHAPTER 1

INTRODUCTION

Semiconductors are of practical importance in an number of connections. Their most direct uses, of course, take advantage of their unique electrical behavior, as in transistor, crystal rectifiers. Closely related to these are the applications which combine electrical and optical effects, as in luminescent material and photoconductors. Furthermore, semiconductors are used in many other ways, in which the connection between their semiconducting behavior and the particular application is much more subtle.

By reason of the very small energy gap and small effective mass of carriers, HgTe is one of the interesting semiconductors whose properties are in the transition region between semiconductors and metals. The first work on HgTe (Nikol, Skaya and Regel 1955) was carried out on pressed samples which have an electron mobility of about 12000 $Cm^2V^{-1}Sec^{-1}$. Several authors investigated the properties of HgTe (Carlson (29), Harman et al. (7), Black et al. (6), Lawson et al. (8), Strauss et al. (2) and so on). Rodot and Triboulet 1962 and Quilliet et al. 1962, discovered that annealing of HgTe in the presence of mercury vapour improved the properties of this material, and it became possible to obtain intrinsic

material with an electron mobility of about 30000 $Cm^2V^{-1}Sec^{-1}$.

In 1961, it was concluded (1) that HgSe and $HgSe_{as}Te_{as}$ are semimetals and it was suggested that HgTe might be likewise. This was later corroborated in measurements of the Hall Coefficient and of electrical resistivity (2) on HgTe and on its alloys, at low concentration with CdTe. These and related experiments were ultimately interpreted (3) in terms of an inverted band structure model derived from that proposed originally by Groves and Paul (4) for grey tin. Independently of ref. (3), Groves and Paul (5) suggested that the inverted band model applies to HgTe as well as - Sn.

Earlier investigators like Black et al. (6), Harman et al. (7) and Lawson et al. (8) on the basis of their electrical measurements estimated HgTe to be a narrow gap semiconductor with an energy gap of-0.01 - 0.025 ev.

On the basis of inverted band structure of HgTe it is estimated (9), (10), (11) and (12) that the energy gap is -0.15 ev at 295 K and is very temperature sensitive. Table (1.1) shows some of the reported band parameters.

Compound	Energy Gap (ev)		Effective Mass(m)		Ref.
	$E_g = E_{\Gamma_6} - E_{\Gamma_7}$	$E_t = E_c - E_v$ (k=0)	Electron m_e (k=0)	Hole m_h	
HgTe	0.01				(8)
	0.02				(7)
	0.025				(6)
	-0.30 (4.2K)	0			(10)
	-0.15 (295 K)				(9,10)
		-.003	.029 (4.2K)	0.35	(11)
		-.02			(12)
			.027(4.2K)		(16)
				0.68	(26)
				0.55	(26)

Table (1.1) Values of some band parameters of HgTe

CHAPTER 2

THEORY

2.1 Hall Effect

One of the most important tools in semiconductors work is the measurement of Hall Effect. Conductivity measurements alone give information about the product of mobility and carrier concentration, (it is discussed later), but do not serve to separate these quantities. The additional information provided by Hall effect measurements enable one to determine these quantities separately.

The experimental arrangement for a Hall effect measurement is shown schematically in figure (2.1). A current, I is passed through the material, and a magnetic field ,B, is applied at right angle to the direction of current flow. A transverse voltage develops, the sign of which, depends on the material being investigated. The voltage is proportional to the current and the field, and inversely proportional to the thickness in the direction of the magnetic field. The proportionality constant is called the Hall Coefficient (R).

$$V = \frac{10^{-8} R I B}{t} \qquad (2.1)$$

Where I is in amperes, B in gauss, t in cm, V in volts, and R in cm^3/coulomb.

By applying the conventional rule to the interaction of the current flow with the magnetic field, it can be seen that for the case shown in figure (2.1), if the material is n- type, electrons flow right to left in the specimen, and tend to move up in the magnetic field. The top develops a negative potential to oppose this motion. For p- type material, holes move from left to right, and also tend to move to the top, which consequently develops a positive potential to oppose any such transverse flow of holes. We see then, that the sign of the Hall coefficient differentiates n, and p type semiconductors.

In the direction of the Hall voltage, the force exerted by the emf just balances the force exerted by the magnetic field on the carriers, thus

$$q\frac{V}{a} = \frac{1}{c}\cdot v_x B \qquad (2.2)$$

(q is electron charge)

where c is the velocity of light, v_x the particle velocity in the x direction (c.g.s. units are used). The current density in x direction is I/ at, so that:

$$-v_x = \frac{I}{nat} \qquad (2.3)$$

where n (or p) is the electron (or hole) density, therefore:

$$\frac{qV}{a} = IB/cnat \qquad (2.4)$$

where all quantities are expressed in c.g.s. units. Converting to practical units and substituting the value of c, we have:

$$V = 10^{-8}\frac{IB}{nqt} \qquad (2.5)$$

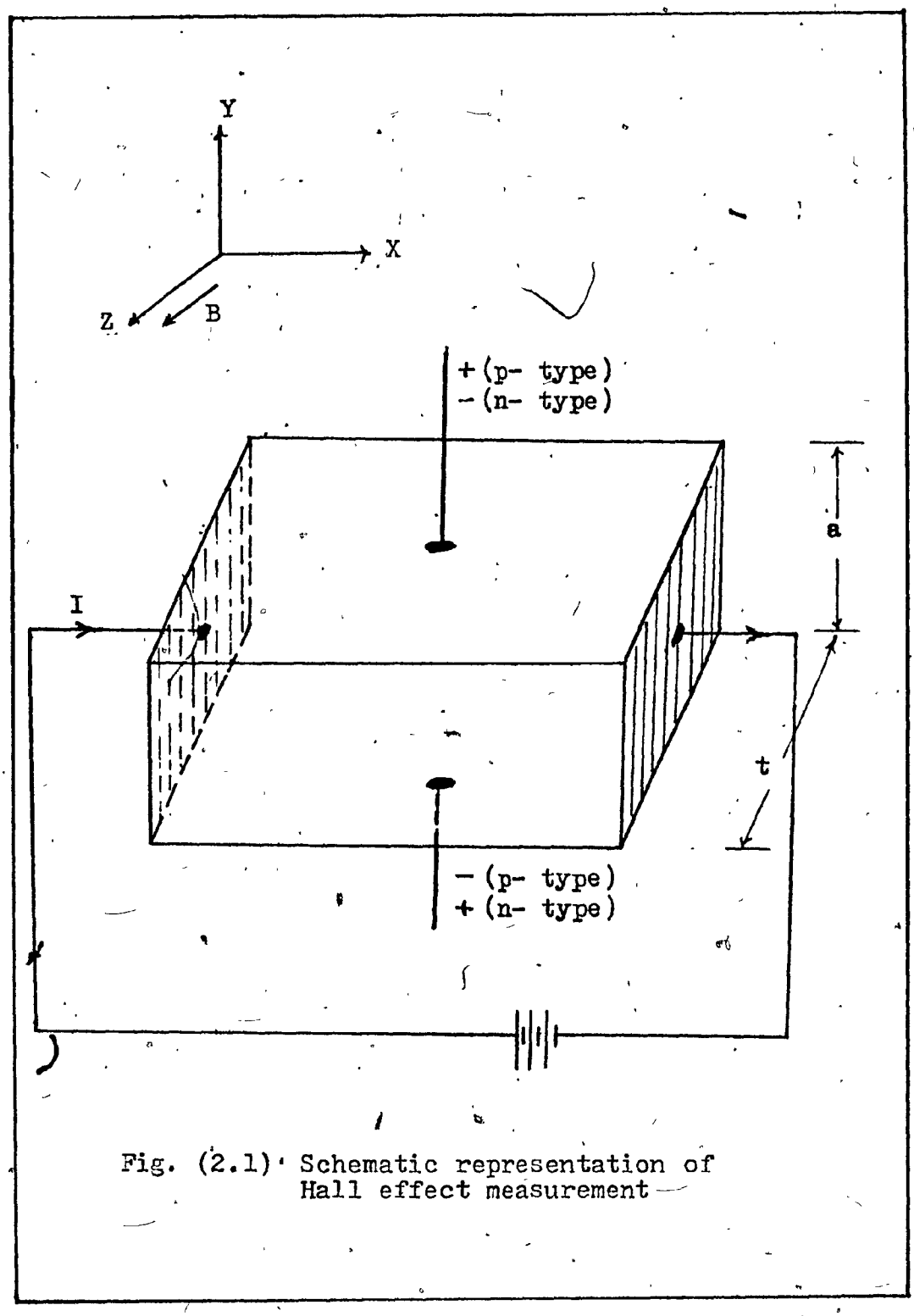

Fig. (2.1) Schematic representation of Hall effect measurement

Comparison with (2.1) shows that:

$$R = -\frac{1}{nq} \tag{2.6}$$

(negative for electrons)

The corresponding expression for hole is

$$R = +\frac{1}{pq} \tag{2.7}$$

(positive for holes)

where $q = -1.60 \times 10^{-19}$ coulomb.

The product of Hall coefficient and conductivity gives the Hall Mobility.

$$\mu = R\sigma$$

2.2 Electrical Conductivity and Hall Mobility

The conductivity provided by conduction electrons will be determined by the number of electrons, and ease of their movement in an applied electric field. The latter is described by their "mobility" which is the drift velocity of the carriers in cm/sec in a field of 1 volt/cm, thus:

$$\sigma_n = \mu_n q n \tag{2.8}$$

where σ_n is the conductivity due to the electrons in $(\text{ohm cm})^{-1}$ μ_n is in $\text{cm}^2/\text{volt sec}$, and q is 1.60 10^{-19} coulomb. The conductivity due to holes is:

$$\sigma_p = \mu_p q p \tag{2.9}$$

and the total conductivity is:

$$\sigma = \frac{1}{\rho} = q\left(\mu_n n + \mu_p p\right) \qquad (2.10)$$

where ρ is the resistivity. Often either n or p predominates and one of the terms on the right hand side of (2.10) may be neglected. In some materials a large difference between μ_n and μ_p produces this result also. The temperature dependence of the conductivity of semiconductors is one of the most striking and characteristic of their properties. The principal change in the conductivity of a given sample, with temperature, result from changes in carrier concentration, although the mobilities also vary with temperature. At low temperatures the conductivity is low, because most of the carriers are frozen out on the donors centers. As the temperature rises the degree of ionization of the donors increases, and the rising carrier concentration as expressed in equation (2.22) results in a rapidly increasing conductivity. At around 100° K the conductivity reaches a maximum, because of complete ionization of the donors.

2.3 Fermi-Dirac Statistics Applied to Semiconductors

In many kind of experiments done on semiconductors, it is of fundamental importance to be able to determine the state of occupancy of the various allowed electronic states. The occupancies depend upon the number and distribution in energy of the allowed states, the position of the Fermi level, and

the temperature. To illustrate how these quantities are related to the occupancy of states, we will consider a semiconductor with a certain density of donor levels, N_D, all at the same energy and a smaller concentration of acceptor levels N_A, also at one energy as in figure (2.2).

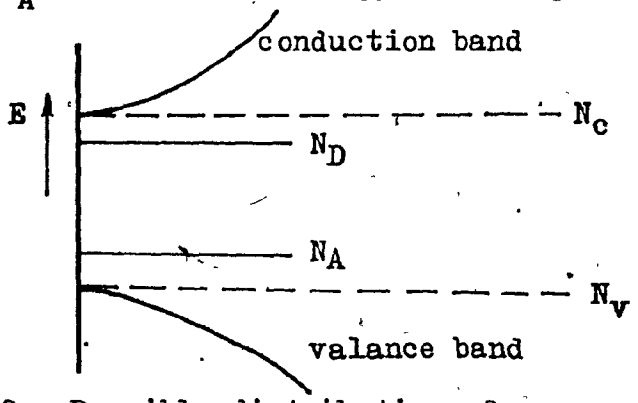

Fig. 2.2 Possible distribution of energy levels for a typical semiconductor.

The first task is to see how the position of the Fermi level can be found. We note that ionized accepters are negatively charged, and that their concentration is $(N_A - p_A)$ where N_A is the total concentration of acceptor centers, and p_A is the concentration of holes on acceptor centers. The total density of negative charges is thus $n + (N_A - p_A)$. Similarly the total density of positive charge is $p + (N_D - n_D)$ where N_D is the density of donor centers, and n_D is the density of electrons on donor centers. The condition of charge neutrality then requires that:

$$n + (N_A - p_A) = p + (N_D - n_D) \qquad (2.11)$$

The total number of electrons in the conduction band and in donor centers is determined by the position of the Fermi level, thus

$$n + n_D = \int f(E)\, N(E)\, dE \qquad (2.12)$$

where F(E) is the Fermi distribution function. The probability of finding an electron in a state of energy E_1 in the conduction band is

$$f(E_1) = \frac{1}{1 + \exp\left[(E_1 - E_F)/kT\right]} \qquad (2.13)$$

where E_F is the Fermi level and k is the Boltzmann's constant. The probability of finding an electron not occuping a state of energy E_2 in the valence band is

$$1 - f(E_2) = \frac{1}{1 + \exp\left[(E_F - E_2)/kT\right]} \qquad (2.14)$$

For a semiconductor with a large energy gap, $(E_1 - E_F)$ and $(E_F - E_2)$ are much greater than kT, and equations (2.13) and (2.14) reduce to :

$$f(E_1) = \frac{1}{\exp\left[(E_1 - E_F)/kT\right]} \qquad (2.15)$$

and

$$1 - f(E_2) = \frac{1}{\exp\left[(E_F - E_2)/kT\right]} \qquad (2.16)$$

The approximation leading to equations(2.15) and (2.16)is not strictly valid in the case of a semimetal, since the energy gap is negative. However it is assumed that no excessive fundamental error is introduced using them, in order to receive the carrier concentrations in closed forms as are expressed in equations (2.17) and (2.18) .

The electron and hole concentrations in the conduction and valence bands are respectively

$$n = N_c \exp\left[(E_F - E_c)/kT\right] \tag{2.17}$$

$$p = N_v \exp\left[(E_v - E_F)/kT\right] \tag{2.18}$$

where E_c and E_v are the band edge energies of the conduction and valence bands respectively. N_c and N_v are the effective density of states given by:

$$N_c = 2\left(2\pi m_e^* kT/h^2\right)^{3/2} \tag{2.19}$$

$$N_v = 2\left(2\pi m_h^* kT/h^2\right)^{3/2} \tag{2.20}$$

where m_e^* and m_h^* are the densities of state effective masses of electrons and holes respectively.

For the intrinsic semiconductors the electron and hole concentrations are equal and the intrinsic carrier concentration n_i is:

$$n_i = n = p \tag{2.21}$$

then

$$n_i^2 = n p = N_c N_v \exp\left(-E_g/kT\right) \qquad (2.22)$$

where $E_g = E_c - E_v$ is the energy gap of the semiconductor.

Now if we consider that the donor atoms and acceptor atoms are not ionized, from the condition of eletrical neutrality, we have:

$$n = p + (N_D - N_A) - N_D f_D + N_A f_A \qquad (2.23)$$

where f_D is the probability that the donor atom is not ionized and f_A is the probability that the acceptor atom is not ionized and

$$f_D = \left\{ 1 + \frac{1}{g_D} \exp\left[(E_D - E_F)/kT\right] \right\}^{-1} \qquad (2.24)$$

f_A is given by a similar expression. In the equation (2.24) E_D is the ground state of the donor impurity center and the factor g_D is the degeneracy of the ground state, and is usually assumed to be 2 . By assuming $n \gg p$, and by using equations (2.17) and (2.24), and knowing $N_D f_D \gg N_A f_A$ equation (2.23) becomes

$$\frac{n(n + N_A)}{N_D - N_A - n} = \frac{N_c}{2} \exp\left[-(E_c - E_D)/kT\right] \qquad (2.25)$$

where $(E_c - E_D)$ is the ionization nergy of the donors.

At very high temperature the intrinsic concentration n_i becomes large compared to $(N_D - N_A)$, and equation (2.23) reduces to $n \simeq p$. The semiconductor becomes intrinsic. As the temperature is lowered, the electron concentration becomes a constant,

$$n \simeq N_D - N_A \tag{2.26}$$

At the very low temperatures when $n \ll N_D$, equation (2.25) becomes:

$$n = \frac{N_D - N_A}{N_A} \cdot \frac{N_c}{2} \cdot \exp\left[-(E_c - E_D)/KT\right] \tag{2.27}$$

2.4 The Band Model of Mercury Telluride

There is considerable evidence that band structure in HgTe corresponds to a model proposed by Groves and Paul (4) for a gray tin. Herman et al. (3) produced a similar explanation in the study of HgTe. The conduction band is at the center of the Broullion Zone degenerate with heavy hole band, belonging together with it to Γ_8 level. The Γ_6 level lies below, thus $E_g = E_{\Gamma_6} - E_{\Gamma_8} < 0$ whereas the energy gap between conduction and valance band $E_g = 0$

The conduction band can be described by a simplified Kane (13) formula:

$$E_c = \frac{\hbar^2 k^2}{2m_0} + \frac{1}{2}\left\{ \left(E_g^2 + \frac{8}{3} p^2 k^2 \right)^{1/2} - |E_g| \right\} \qquad (2.28)$$

$$E_{V_2} = \frac{\hbar^2 k^2}{2m_0} - \frac{E_g}{2} - \frac{1}{2}\left[E_g^2 + \frac{8}{3} p^2 k^2 \right]^{1/2} \qquad (2.29)$$

that, $E_g = E_{\Gamma_6} - E_{\Gamma_8}$

where E_c, and E_{V_2}, are the energies in the conduction band, and light hole valance band respectively, E_g, is the principal band gap at $k = 0$, p is the Kane's momentum matrix

element, $\hbar$ is Plank's constant/ 2π , and m_o is the electronic rest mass.

The validity of Kane's formula for HgTe has been checked experimentally by W. Szvmanska (15) and S.H. Groves et al. (16). It has been pointed out by Groves (17) that the "effective mass energy gap" is not valid in the case of HgTe. It can be shown (18) that the electron concentration in the conduction band, n is given by:

$$n = \frac{\sqrt{2}}{\pi^2}\left(m_e^{(4)}\frac{4\pi^2 kT}{h^2}\right)^{3/2}\left[F_{1/2}(\gamma)+\beta\left(5/2-5f\right)F_{3/2}(\gamma)\right.$$
$$\left.+\beta^2\left(1-\frac{21}{2}f\right)F_{5/2}(\gamma)-4f\beta^3F_{7/2}(\gamma)\right] \qquad (2.30)$$

where $\beta=\frac{kT}{|E_g|}$, $f=\frac{m_e^*}{m}$, $\gamma=\frac{E_F}{kT}=\frac{3h|E_g|}{16\pi^2p^2}$

k is Boltzmann's constant, E_F is the Fermi level relative to the bottom of the conduction band, and m_e^* is the band curvature effective mass of the electron at the edge of the conduction band, $F_j(\gamma)$ is the Fermi-Dirac integral of order j.

$$F_j(\gamma)=\int_0^\infty \frac{\varepsilon^j d\varepsilon}{1+\exp(\varepsilon-\gamma)} \qquad (2.31)$$

The carrier concentration in the heavy hole valance band V_1 is given similarly by the well-known expression (1).

$$p=\frac{\sqrt{2}}{\pi^2}\left(m_h^*\frac{4\pi^2 kT}{h^2}\right)^{3/2}F_{1/2}\left(-\gamma-\frac{E_t}{kT}\right) \qquad (2.32)$$

where m_h^* is the density of state effective mass in the heavy hole band and E_t, the thermal gap, is defined as:

$$E_t = E_c - E_{v_1}$$

It has been shown, however, that band parameters of pure HgTe are strongly temperature dependent. Piotrzkowski and Porowski (18) show that transition from negative to positive E_o can be induced by temperature at an external pressure of about 10 K atom.

Comparing band structure of InSb with of HgTe one can see that the ordering of the Γ_6 and Γ_8 is inverted, for this reason we call it inverted band model. Band model of InSb and HgTe are shown in Figures (2.3) and (2.4) respectively.

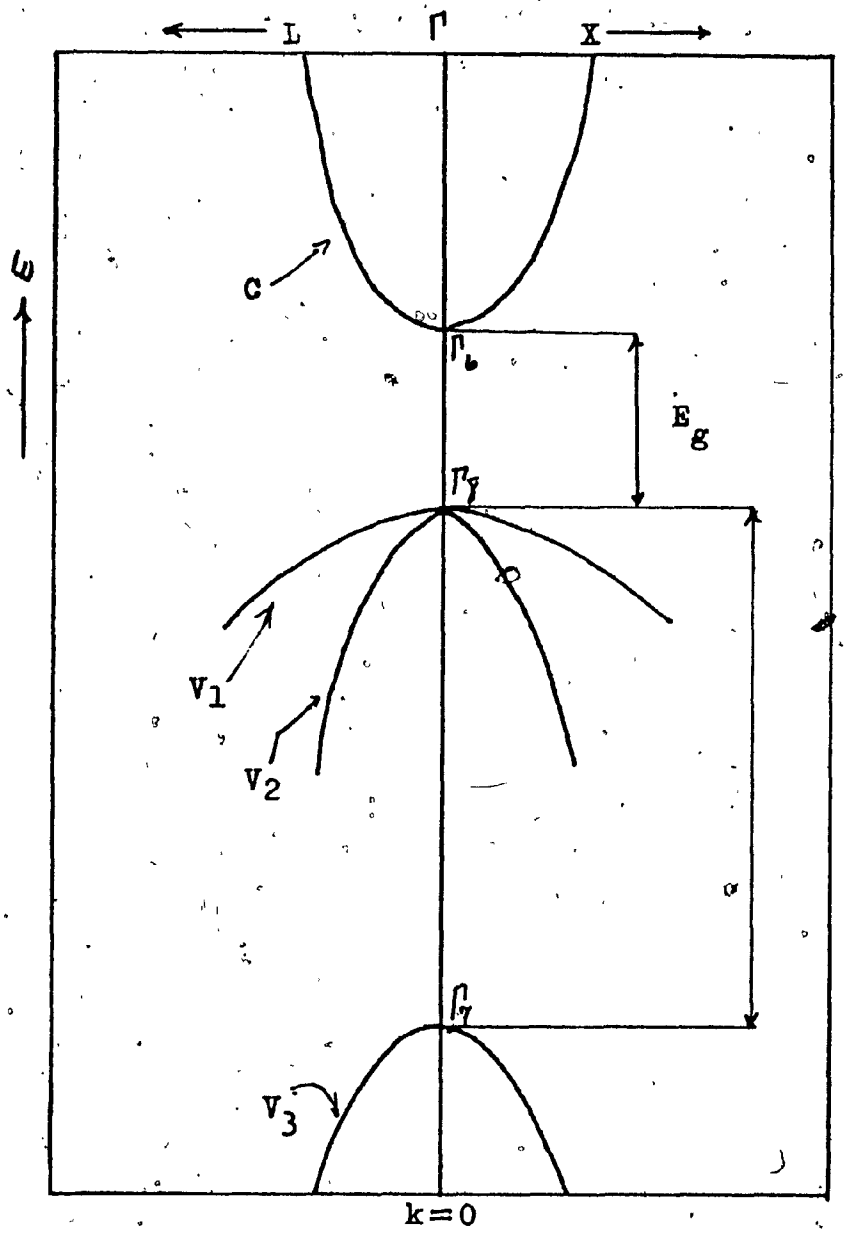

Fig. (2.3) The energy band diagram of InSb

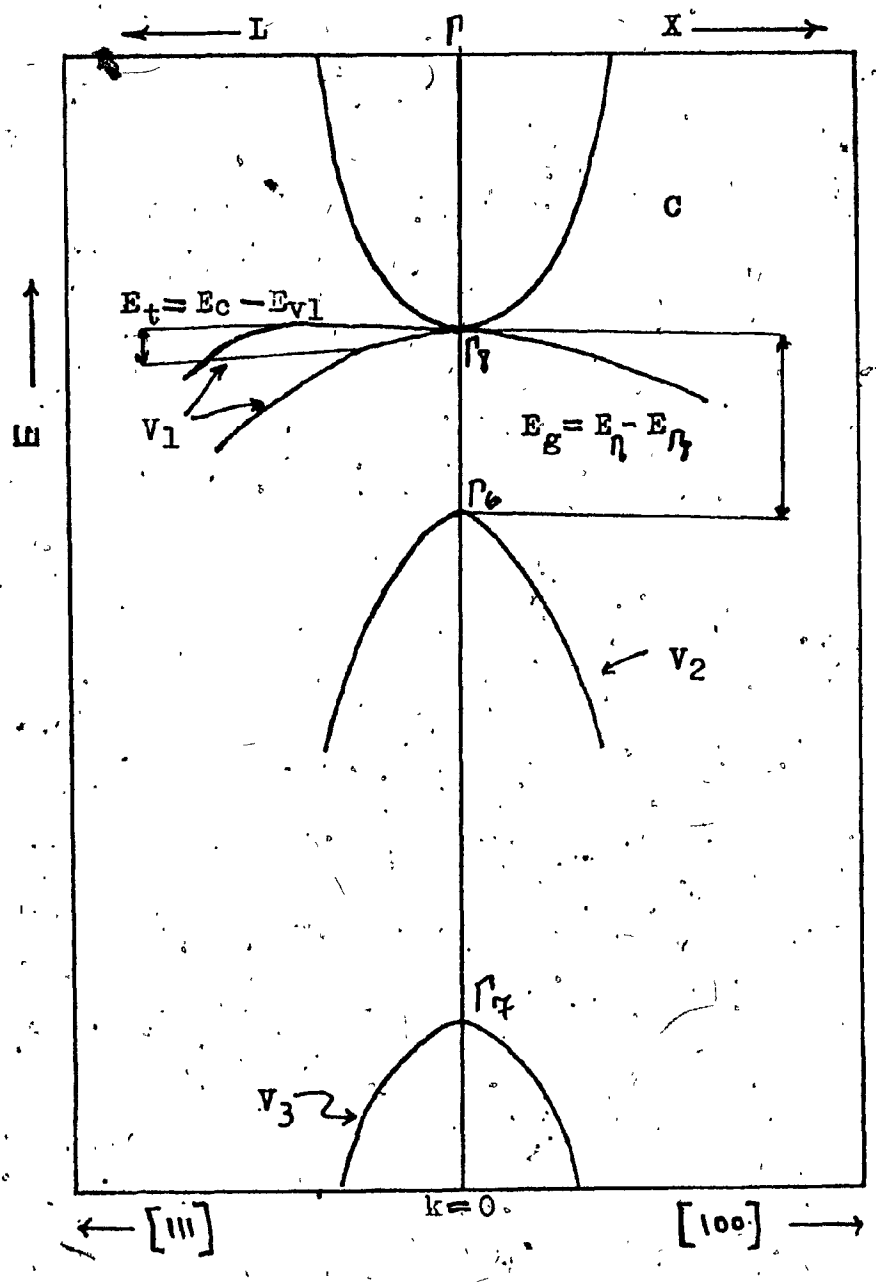

Fig. (2.4) The Inverted Band Model of HgTe

CHAPTER 3

EXPERIMENTAL EQUIPMENT

3.1 Sample Preparation and Geometry

The mercury telluride crystals were prepared by the Bridgman technique, in the solid - state lab. of electrical engineering department.

The shape of the sample which has been most extensively studied, is a rectangular parallelopiped with the ends completely covered with highly conducting material to ensure parallel current lines. It is essential that the length to width ratio of the sample to be greater or equal to 4 , since a smaller ratio will produce shorting effect of the Hall field. A good discussion of this effect is given by Beer (20). The dimensions of the samples were chosen according to the ASTM standards. (21)

Slices of single crystal of approximately 1 to 2 mm thick were cut by means of a wire saw specially designed by Dr. B.A. Lombos of the electrical engineering department. Those were then fixed on a base by using melting wax and lapping to a uniform thickness with alumina powder. After lapping the samples were cleaned and degreased by boiling in trichloroethylen and acetone several times. The samples were then chemically polished in Br and methanol. For this purpose

the solution of 1% Br and methanol is used for not more than 30 seconds.

Contacts to the samples were made by indium solder and then connected to the sample holder by thin gold wire. The contact is made just before the experiment, since a reaction of indium solder with HgTe for a long period was reported (22).

The dimensions of the samples were measured by a travelling microscope having an accuracy of 0.01 mm. The contacts were checked by using a curve tracer to ensure ohmic contact. Figure (3.1) shows the assembly of the sample.

3.2 Experimental Apparatus

3.2.1 The Sample Holder

A schematical of the sample holder is shown in figure (3.2). The sample is held on a brass plug. The heater consists of approximately 45Ω nichrome wire which is wrapped around the top section of the plug. The wire is insulated electrically from the plug by using mica sheets and epoxy, and the sample insulated from the plug by a piece of P.V.C. board. All wires ($\simeq$ 16) are led to a measurement system and a power supply by a phenolic rod and a receptable block. An O ring is provided around the block to vacuum seal the sample chamber.

The sample temperature is controlled by a platinum resistance thermometer for temperatures greater than 20 K and a germanium resistance thermometer for less than 20 K. The sample is held on the plug by two brass screws, and a small amount of vacuum grease is used for thermal contact.

3.2.2 The Cryostat and Electromagnet

The schematic drawing of the cryostat is shown in figure (3.3).

The sample is placed at the bottom of the sample chamber. The portion of the sample chamber in which the sample is positioned is thermally shielded by a radiation shield. This shield is cooled by the liquid nitrogen. A pressure of less than 10^{-5} mmHg is maintained in the vacuum chamber by means of a mechanical and an oil diffusion pump. The vacuum chamber insulates the sample chamber from the outer shell of the cryostat.

The low temperatures inside the sample chamber are maintained by using liquid nitrogen or liquid helium, and the heater which was mentionned previously. The sample chamber is vacuumed by a rotary pump and before admitting the liquids, the chamber is dried by flushing with helium gas several times. The temperature inside the chamber is maintained by a temperature control system within 0.5 K over the entire temperature range.

The magnetic field for measurement the Hall effect is provided by a 12-inch Varian (3603 electromagnet). The field is controlled by a rotary switch located on the control panel. The reverse field is provided by an inverting switch. The maximum field intensity available is about 10 K Gauss.

3.2.3 Measurement System

The schematic drawing of the electrical wiring and measurement equipment is shown in figure (3.4).

The 50 mA Hall sample current was supplied by a constant current source (Harrison 6209B DC power supply, Hewlett - Pachard). The direction of the current could be reversed by a reversing switch. A selector switch was used to measure the voltage between each pair of contacts.

The heater around the sample holder was heated by a current of maximum 0.2 Ampere. A current of 10μA was used with the platinum resistance thermometer, and a current of 1μA was used with the germanium resistance thermometer. The 10μA and 1μA currents were supplied by a power supply constructed in the physics workshop. The temperature was controlled by a John Fluke, MFG, DC differential voltmeter model 881A. The Hall voltages were measured by Hewlett - Pachard digital voltmeter.

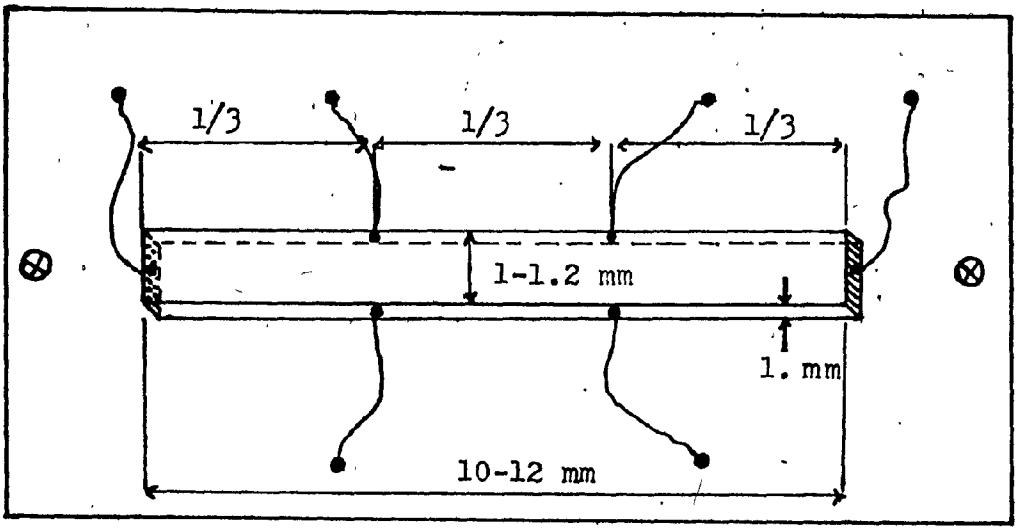

Fig. (3.1) Assembly of the HgTe sample

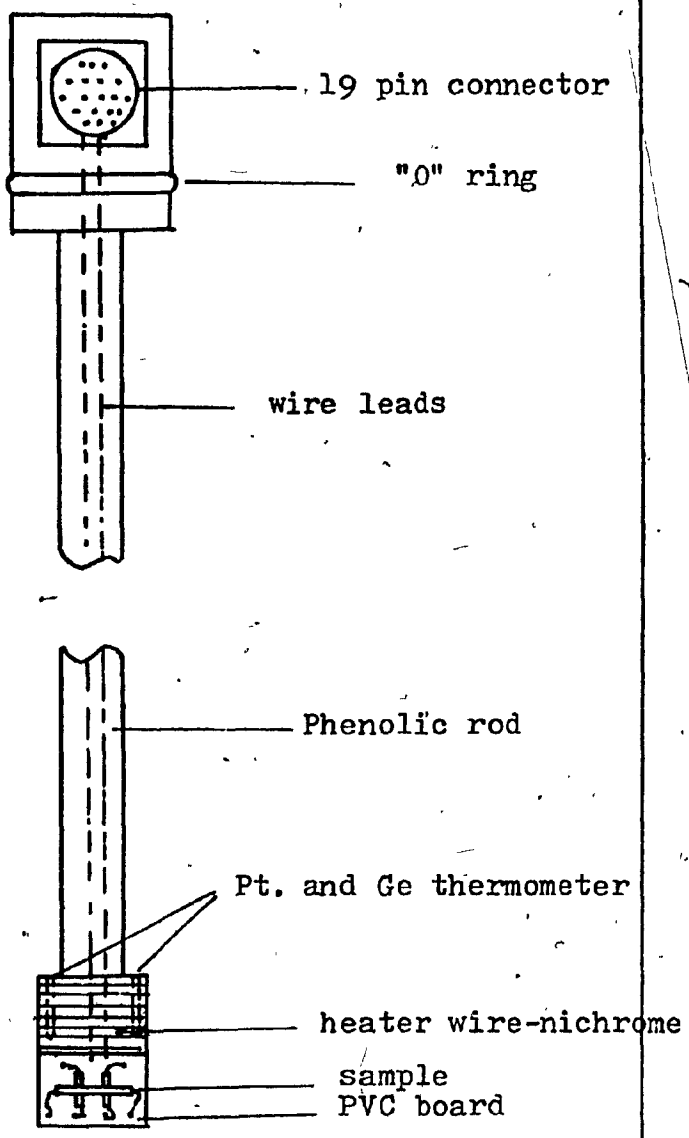

Fig. (3.2) Schematic drawing of sample holder

LEGEND

A Electrical Connectors
B Off-Gas Line
C Helium Fill & Vent
D Insulation Line
E Nitrogen Vent
F Outer Shell
G Nitrogen Reservoir
H Helium Well
I Insulation Space
J Outer Tail Section
K Nitrogen Temperature Radiation Shield
L Sample Heater
M Exchange Gas Chamber
N Capillary
O Throttle Valve
P Sample Support Tube
Q Throttle-Valve Stem
R Nitrogen Fill
S Helium Gauge Port
T Throttle-Valve Top Works

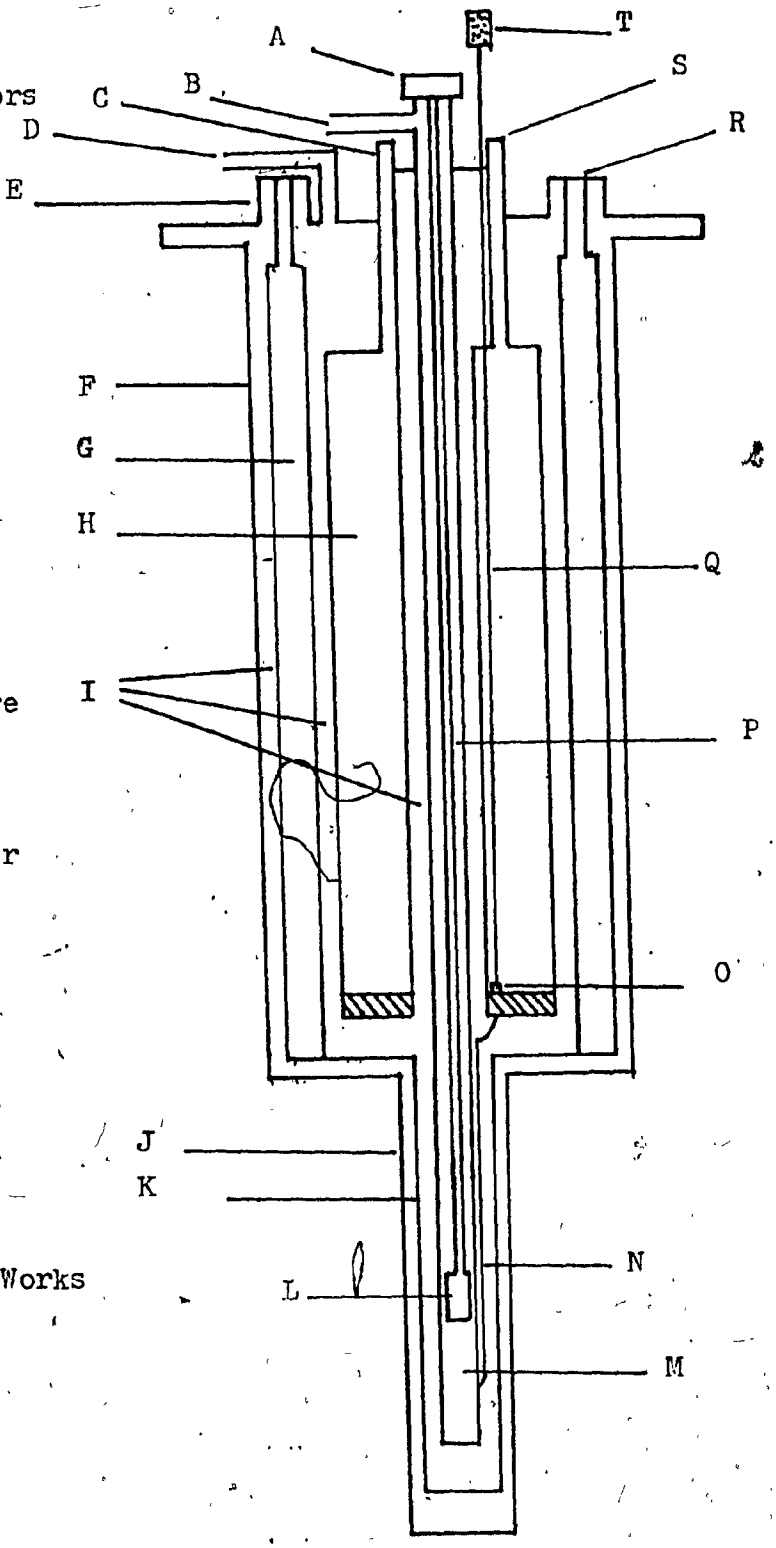

Fig. (3.3) Schematic drawing of the low temperature cryostat

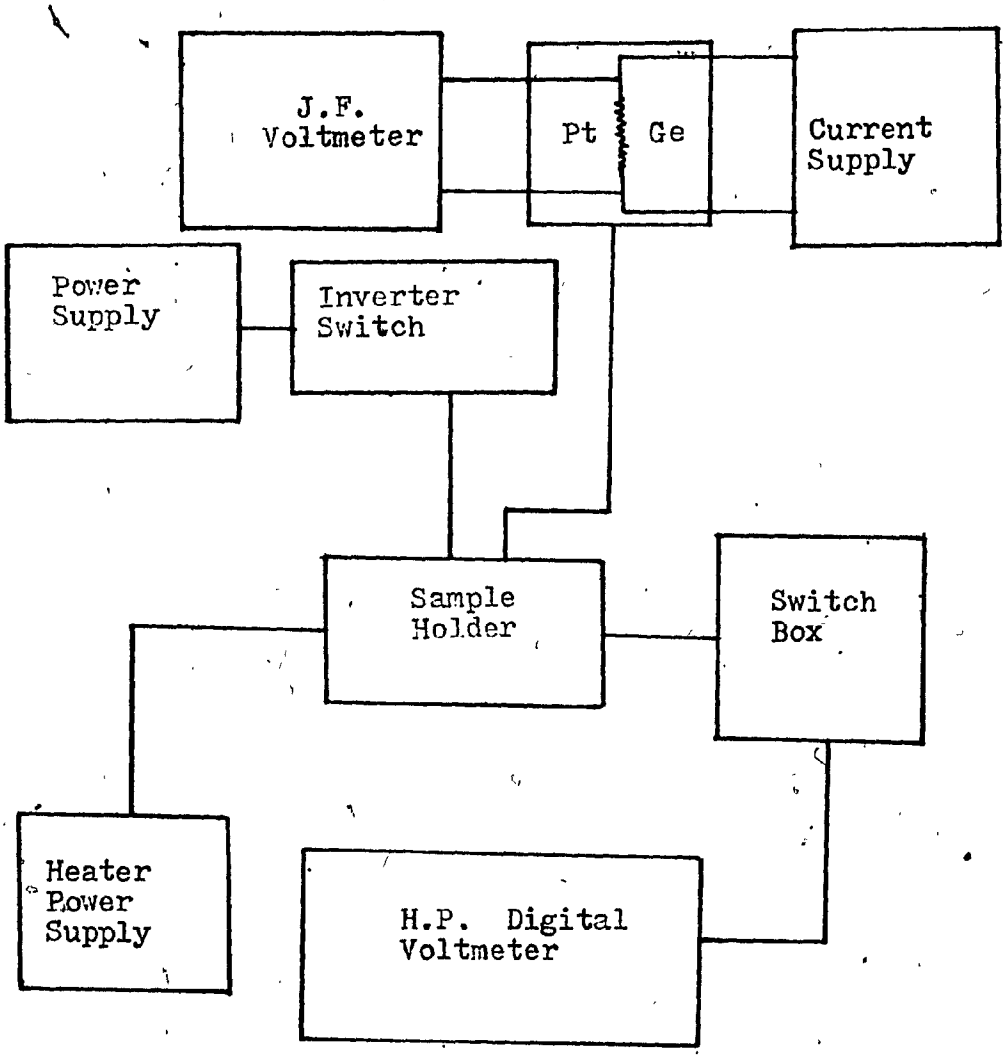

Fig. (3.4) Block diagram and measurement equipment

CHAPTER 4

MEASUREMENT PROCEDURE

4.1 Hall Coefficient Measurement

The specimen was placed in its position inside the sample chamber. The sample was connected in the electrical circuit as in figure (4.1). A magnetic field of 5000 gauss and a sample current of 50 mA were provided. The potential drop in position 3, (V_3 (I,B)) and position 5, (V_5 (I,B)) were measured by means of the selector switch at various temperatures.

In order to check the stability of the current, the above voltages were remeasured. A difference of % 0.5 between the two measurements was observed. By reversing the direction of current and inverting the magnetic flux polarity, the potential drops of (V_3 (-I,B)), (V_5 (-I,B)), (V_3 (I,-B)), (V_5 (I,-B)), (V_3 (-I,-B)) and (V_5 (-I,-B)) were determined.

By inserting liquid nitrogen or helium inside the sample chamber, low temperatures were achieved. To avoid shocking the contacts the temperature was lowered slowly. Then by passing a current (maximum 0.2 Ampere) through the heater on the sample holder the temperature of the sample was increased, and all the above measurements were repeated for various temperatures.

The data obtained was used to calculate:

$$R_{H_3} = 2.5 \times 10^7 \frac{t}{4BI} \left(V_3(I,B) + V_3(I,-B) + V_3(-I,B) + V_3(-I,-B) \right)$$

$$R_{H_5} = 2.5 \times 10^7 \frac{t}{4BI} \left(V_5(I,B) + V_5(I,-B) + V_5(-I,B) + V_5(-I,-B) \right)$$

where

$$R_{H_{av}} = \frac{R_{H_3} + R_{H_5}}{2} \quad Cm^3 Coul^{-1}$$

where units of V_3 and V_5 are volts, t, the thickness of sample is in cm, B, the magnetic flux is in gauss, and I, the sample current is in ampere.

4.2 Resistivity and Hall Mobility Measurements

By removing the magnetic flux and maintaining the 50 mA current passing along the sample, the potential drops in positions 2 , (V_2 (I)), and 4 , (V_4 (I)), were obtained. By reversing the current polarity (V_2 (-I)) and (V_4 (-I)) were determined.

The electrical resistivity of the samples was calculated as:

$$\rho_A = \frac{wt}{2dI} \left(V_2(I) + V_2(-I) \right)$$

$$\rho_B = \frac{wt}{2dI} \left(V_4(I) + V_4(-I) \right)$$

that

$$\rho_{av} = \frac{\rho_A + \rho_B}{2} \quad \text{(ohm cm)}$$

where w , t , and d, the width , thickness and arm's spacing of sample, respectively, are in Cm , I, the sample current, is in ampere.

The Hall mobility of sample was calculated from:

$$\mu_H = \frac{R_H}{\rho} \qquad (cm^2\ V^{-1}\ S^{-1})$$

4.3 A Procedure to Eliminate Certain Associated Effects in Hall Voltage Measurement

In order to obtain accurate Hall voltage measurement certain associated effects which give rise to voltage drops at the Hall probes must be eliminated. A parallelepiped sample shape is chosen to describe these effects. As the physical size of the Hall sample is usually very small (1 X 0.1 X 0.2 cm, typical size) it is extremely difficult to align the Hall probes properly. Figure (4.2a) shows the equipotential lines along the sample when it is subjected to a current at its ends. Because of the misalignment the Hall probes, A and D are at different potentials. This potential drop across the probes is known as the "IR drop". It is dependent on the direction of the current but, is independent of the magnetic field.

The electrons which constitute the sample current do not move across the sample with the same velocity. The faster electrons will follow a different path when a magnetic field with intensity B is applied perpendicular to the sample than the slower electrons. Hence more energy will be transported to one side of the sample than the other, resulting in a temperature difference, $T_A - T_D$, as shown in figure (4.2b). This effect is known as the Ethingshausen effect. Since the Hall probes and the sample are of different materials, they form a thermocouple and thus generating a potential across the sample.

When the two ends of the Hall sample are subjected to a temperature difference a thermal current will flow across the sample as shown in figures (4.2c) and (4.2d). In the Nernst effect a potential, V_N, will appear across the sample when a magnetic field is applied perpendicular to the sample. Under these same conditions a temperature difference across the sample is also produced. This is known as the Righi - Leduc effect.

Because of all these effects the voltage measured across the Hall probe, is the sum of V_H, the Holl voltage, V_{IR}, the voltage due to probes misalignment, V_E, the voltage due to the Ettingshausen effect, V_N, the voltage due to Nerst effect, and V_{RL}, the voltage due to Righi - Leduc effect. All of these voltages with the exception of V_E, can be eliminated by taking a series of measurements with all possible combination of current, I, and magnetic field, B, direction. Noting that V_H and V_E, are dependent on both I and B, V_N and V_{RL} are dependent only on B, and V_{IR} is dependent only on I, the measurements will give, for:

$$(+B,+I): \quad V_1 = V_H + V_E + V_N + V_{RL} + V_{IR}$$

$$(+B,-I): \quad V_2 = -V_H - V_E + V_N + V_{RL} - V_{IR}$$

$$(-B,-I): \quad V_3 = V_H + V_E - V_N - V_{RL} - V_{IR}$$

$$(-B,+I): \quad V_4 = -V_H - V_E - V_N - V_{RL} + V_{IR}$$

Hence,

$$\frac{V_1 - V_2 + V_3 - V_4}{4} = V_H + V_E$$

The Ettingshausen effect can be minimized by immersing the Hall sample in a high thermal conductivity medium. Under this condition V_E, is usually very small and is generally neglected. Some related magnitudes of these effects are given by Smith (23).

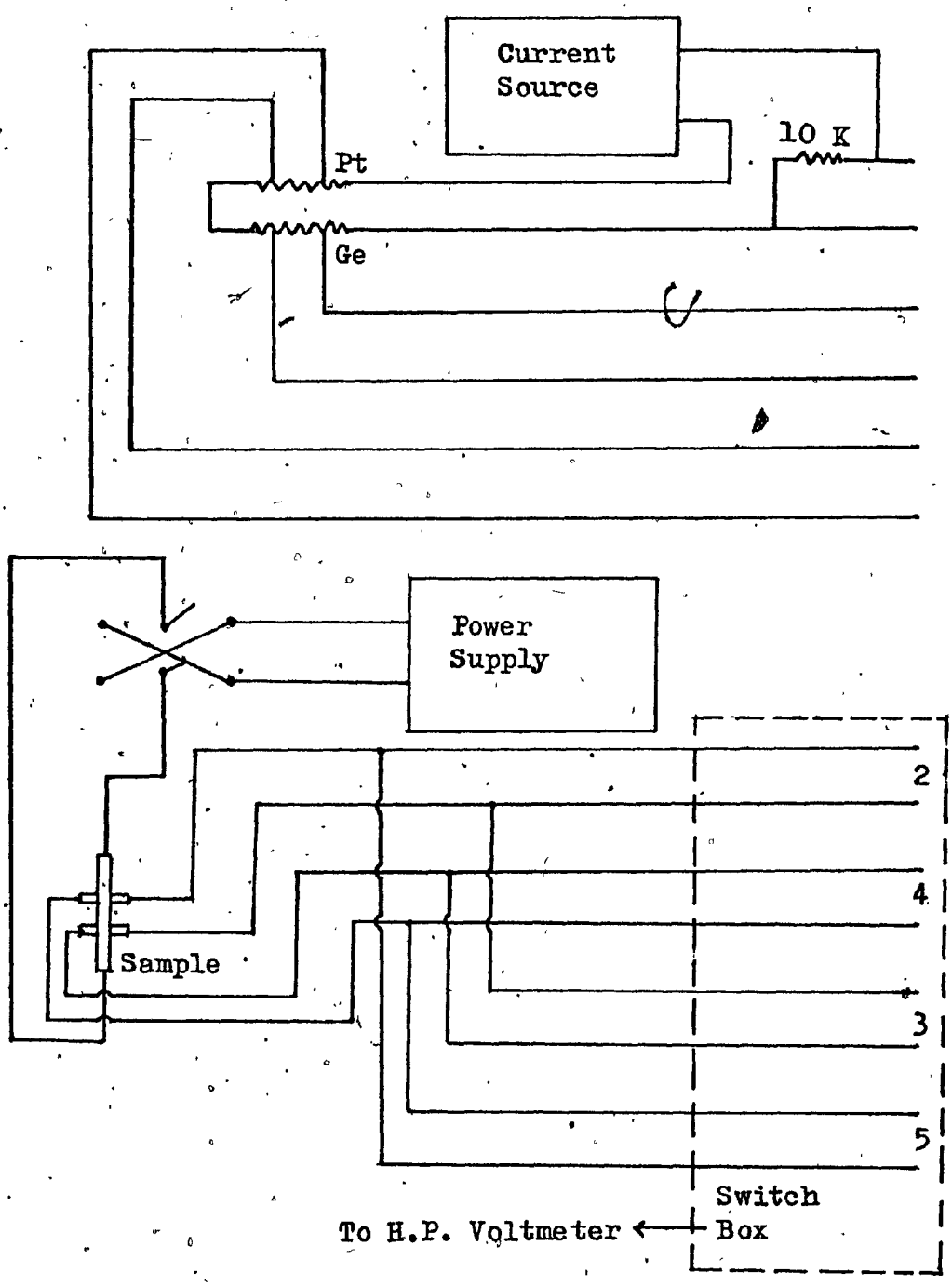

Fig. (4.1) Electrical circuit for Hall effect measurement

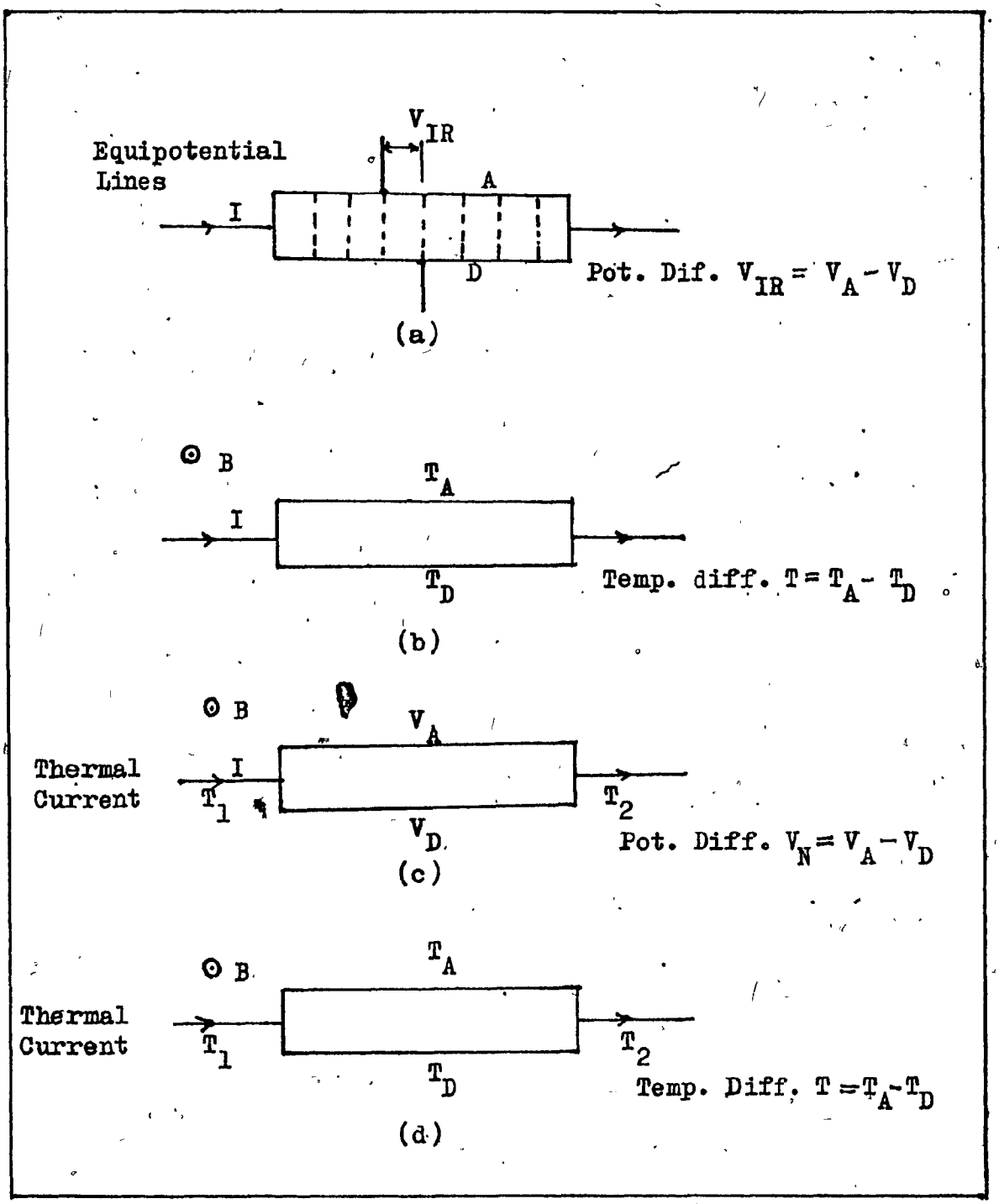

Fig. (4.2) Associated effects present in Hall voltage measurement

CHAPTER 5

EXPERIMENTAL RESULTS

All measurements including Hall Coefficient, Electrical resistivity and Hall mobility were determined from a total four HgTe samples which were fabricated prior to the commencement of the experiments.

Two samples were characterized at very low temperatures by using liquid helium, and two others in nitrogen liquid. A sample current of 50 mA and a magnetic field intensity of 5 KG were used for all samples. The variation of Hall voltage versus magnetic field was also measured.

The Hall Coefficient as a function of reciprocal temperature of three unannealed specimens is shown in figures (5.1) and (5.2). It is deduced from comparing the shape of curves with the results of previous workers, that all samples are n - type. The absolute value of R_H , increases as temperature increases, passing though a maximum at about 135 K before reaching the intrinsic region. The carrier concentration of 10^{20} (cm^{-3}), is calculated at 100 K from $R = 3\pi/8 \times 1/ne$ (a typical formula for n type materials).

Figure (5.3) shows the variation of Hall coefficient versus reciprocal temperature of an annealed sample. The sample is annealed with mercury vapour under pressure of 2.07 K

pascal, at 250° K, for 5 days. The calculations show that, the vacancy concentration of the sample was reduced, and as a result, the carrier concentration is increased.

Figures (5.4) and (5.5) show the electrical resistivity of samples as a function of temperature. The curves of the resistivity of HgTe decreases as temperature increases for temperatures above 50° K and the resistivity is independent of temperature for lower temperatures (between 4.2° K to 50° K). This shows that the conduction processes in these materials are dominated by ionized impurities in the low temperature range.

An expected value of energy gap E_g of about-0.01 ev was obtained from the slope of linear part of the electrical resistivity curves.

Figures (5.6), (5.7) and (5.8) show the Hall Mobility variation of the samples versus temperature. All mobility curves show that the Hall mobility of the samples increases as temperature increases. The low magnitude of Hall mobility (about 3×10^3) $cm^2V^{-1}S^{-1}$ at room temperature indicates that the vacancy concentration of the samples is very high. By annealing the sample, the Hall mobility improved and a value of 6×10^3 $cm^2V^{-1}S^{-1}$ (sample D) at room temperature is achieved.

5.1 Interpretation of Results

Since the proportion of hole concentration to electron concentration is very small, then, the density of intrinsic carrier, n , is given by $n = 3\pi/8 \times 1/Re$. Table (5.1) shows

that variation of n versus temperature, and since $\frac{n}{T^{3/2}} = B\, e^{-\Delta E/2kT}$ a plot of $\ln \frac{1}{RT^{3/2}}$ versus $1/T$ should be linear and yield an accurate value of the energy gap. Figure (5.9) shows this linearity and a value of E_g = 0.03 ev for energy gap is obtained.

5.1.1 Magnetic Field Dependence of Hall Coefficient

In order to characterize different carriers in HgTe the variation of Hall Coefficient as a function of field intensity, and "Two Band Model" is investigated. Figure (5.10) shows the Hall Coefficient (R) versus magnetic field, (B), at 77°K. The curves show the change of R, at high magnetic field (above 1000 gauss) is slightly, but as the magnetic field decreases, the Hall coefficient increases. In these experiments the Hall coefficient at zero field intensity (R_o) were calculated by applying a secular equation treatment, instead of extrapolated from the experimentally curves.

5.1.2 Application of the Two Band Model

It is shown that $R_o/(R_o - R_B)$ is linear function of B^{-2}, and the parameters of the separate bands can be determined from the slope and intercept value of such graphs, figures (5.11) and (5.12).

It is shown (24) that for two isotropic independent bands the variation of R and ρ with B can be expressed in terms of the Hall coefficients, R_1 and R_2, and conductivities σ_1, and σ_2 for the separate bands as:

$$R(B) = \frac{(R_1\sigma_1^2 + R_2\sigma_2^2) + R_1R_2\sigma_1^2\sigma_2^2(R_1+R_2)B^2}{(\sigma_1+\sigma_2)^2 + \sigma_1^2\sigma_2^2(R_1+R_2)^2B^2} \qquad (5.1)$$

$$f(B) = \frac{(\sigma_1+\sigma_2) + \sigma_1\sigma_2(\sigma_1R_1^2 + \sigma_2R_2^2)B^2}{(\sigma_1+\sigma_2)^2 + \sigma_1^2\sigma_2^2(R_1+R_2)^2B^2} \qquad (5.2)$$

for B equal to zero, equations (5.1) and (5.2) becomes:

$$R(0) = R_o = \frac{R_1\sigma_1^2 + R_2\sigma_2^2}{(\sigma_1+\sigma_2)^2} \qquad (5.3)$$

$$f(0) = f_o = \frac{1}{\sigma_o} = \frac{1}{\sigma_1+\sigma_2} \qquad (5.4)$$

From the above equations we can deduce:

$$\frac{f_o}{\Delta f} = tB^{-2} + u \qquad (5.5)$$

$$-\frac{R_o}{\Delta R} = sB^{-2} + a \qquad (5.6)$$

where $\Delta f = f(B) - f_o$, $\Delta R = R(B) - R_o$, and the parameters t, u, s, and a, can be related to the parameters

R_1 and σ_1 of band No. 1, as follows:

$$t = \frac{\sigma_0 - \sigma_1}{\sigma_1 \left(R_0\sigma_0 - R_1\sigma_1 \right)^2} \tag{5.7}$$

$$V = \frac{\sigma_1 \left(R_0\sigma_0 + R_1\sigma_0 - 2R_1\sigma_1 \right)^2}{\left(\sigma_0 - \sigma_1 \right)\left(R_0\sigma_0 - R_1\sigma_1 \right)^2} \tag{5.8}$$

$$s = \frac{R_0\sigma_0 \left(\sigma_0 - \sigma_1 \right)^2}{\sigma_1^2 \left(R_0\sigma_0 + R_1\sigma_0 - 2R_1\sigma_1 \right)\left(R_0\sigma_0 - R_1\sigma_1 \right)^2} \tag{5.9}$$

$$a = \frac{R_0\sigma_0 \left(R_0\sigma_0 + R_1\sigma_0 - 2R_1\sigma_1 \right)}{\left(R_0\sigma_0 - R_1\sigma_1 \right)^2} \tag{5.10}$$

To solve for R_1, and σ_1, only two of the above equations are required. For various combinations of these equations, analytical forms of solution can be obtained. Here we only consider the two equations of s, and a, and give a solution for R_1, σ_1, R_2, and σ_2.

Equation (5.6) can be rewritten in the form of a series of equations:

$$SA_i - SR_0 B_i^{-2} + a R_i = -V \tag{5.11}$$

where

$$A_i = B_i^{-2} R_i \quad , \text{and} \quad U = R_\circ (1-a) \tag{5.12}$$

where i=1, 2 and 3, taken from the experimental curves. To obtain nontrivial solutions the secular determinant, formed from the set of secular equations (5.11), must be different from zero, thus:

$$D = -\begin{vmatrix} A_1 & -B_1^{-2} & R_1 \\ A_2 & -B_2^{-2} & R_2 \\ A_3 & -B_3^{-2} & R_3 \end{vmatrix} \neq 0 \tag{5.13}$$

then we will have:

$$S = -\begin{vmatrix} 1 & -B_1^{-2} & R_1 \\ 1 & -B_2^{-2} & R_2 \\ 1 & -B_3^{-2} & R_3 \end{vmatrix} \frac{U}{D} = -\frac{U}{D}|1| \tag{5.14}$$

$$SR_\circ = -\begin{vmatrix} A_1 & 1 & R_1 \\ A_2 & 1 & R_2 \\ A_3 & 1 & R_3 \end{vmatrix} \frac{U}{D} = -\frac{U}{D}|2| \tag{5.15}$$

and

$$a = \begin{vmatrix} A_1 & -B_1^{-2} & 1 \\ A_2 & -B_2^{-2} & 1 \\ A_3 & -B_3^{-2} & 1 \end{vmatrix} \frac{U}{D} = \frac{U}{D}|3| \tag{5.16}$$

It can be concluded that:

$$R_o = \frac{|2|}{|1|} \tag{5.17}$$

$$a = R_o \frac{|3|}{D\,(1 + R_o |3| D^{-1})} \tag{5.18}$$

and

$$S = \frac{R_o (1-a)|1|}{D} \tag{5.19}$$

Now the one band contributions to the Hall coefficient and conductivity can be determined, as follows:

$$\sigma_1 = \tfrac{1}{2}\sigma_o \left[1 + \left(\frac{E}{E+4}\right)^{1/2}\right] \tag{5.20}$$

with $$E = \frac{-(sa)^{1/2}}{R_o a_o}\left[R_o \sigma_o + \left(\frac{a}{s}\right)^{1/2}\right]^2$$

$$R_1 = \frac{1}{2\sigma_1 - \sigma_2}\left[R_o \sigma_o + \frac{\sigma_o - \sigma_1}{\sigma_1}\left(\frac{a}{s}\right)^{1/2}\right] \tag{5.21}$$

$$\sigma_2 = \sigma_o - \sigma_1 \tag{5.22}$$

$$R_2 = \frac{R_0\sigma_0^2 - R_1\sigma_1^2}{(\sigma_0 - \sigma_1)^2} \qquad (5.23)$$

Now the concentrations n_1, n_2, (fast and slow electrons respectively) and the mobilities μ_1, and μ_2, characterizing the two types of carriers can be evaluated through well-known expressions.

The results of calculations with the values of the band parameters a, and s, of the four crystals is shown in table (5.2). Samples No. 3 and 4, are annealed as mentionned in previous chapter. As it is clear from the table, for annealed samples the mobility of heavy carriers is increased, whereas, the corresponding carrier concentrations are decreased, and so the vacancy concentrations as discussed before, is decreased.

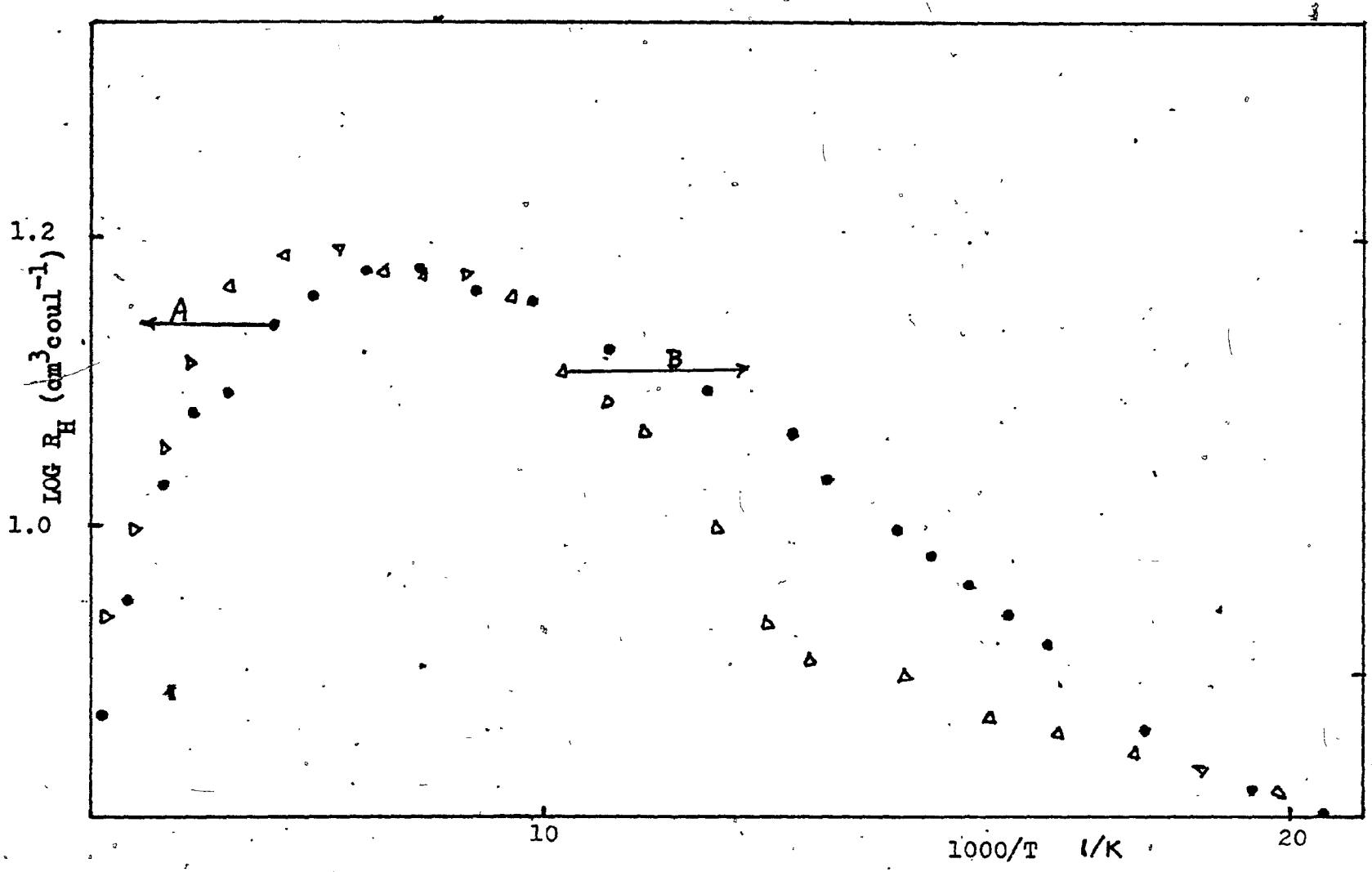

Fig. (5.1) Hall Coefficient as a function of temperature

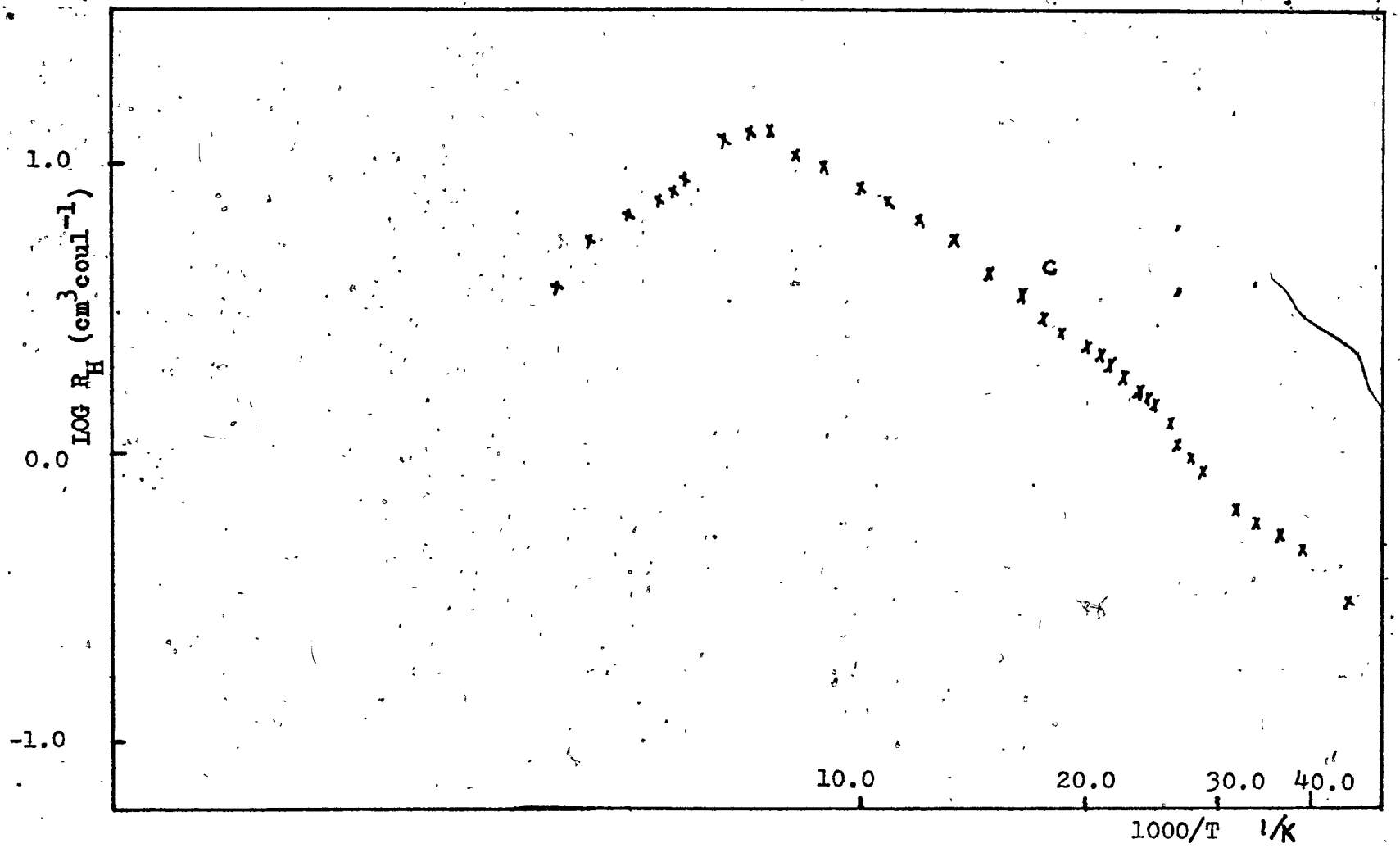

Fig. (5.2) Hall Coefficient as a function of temperature

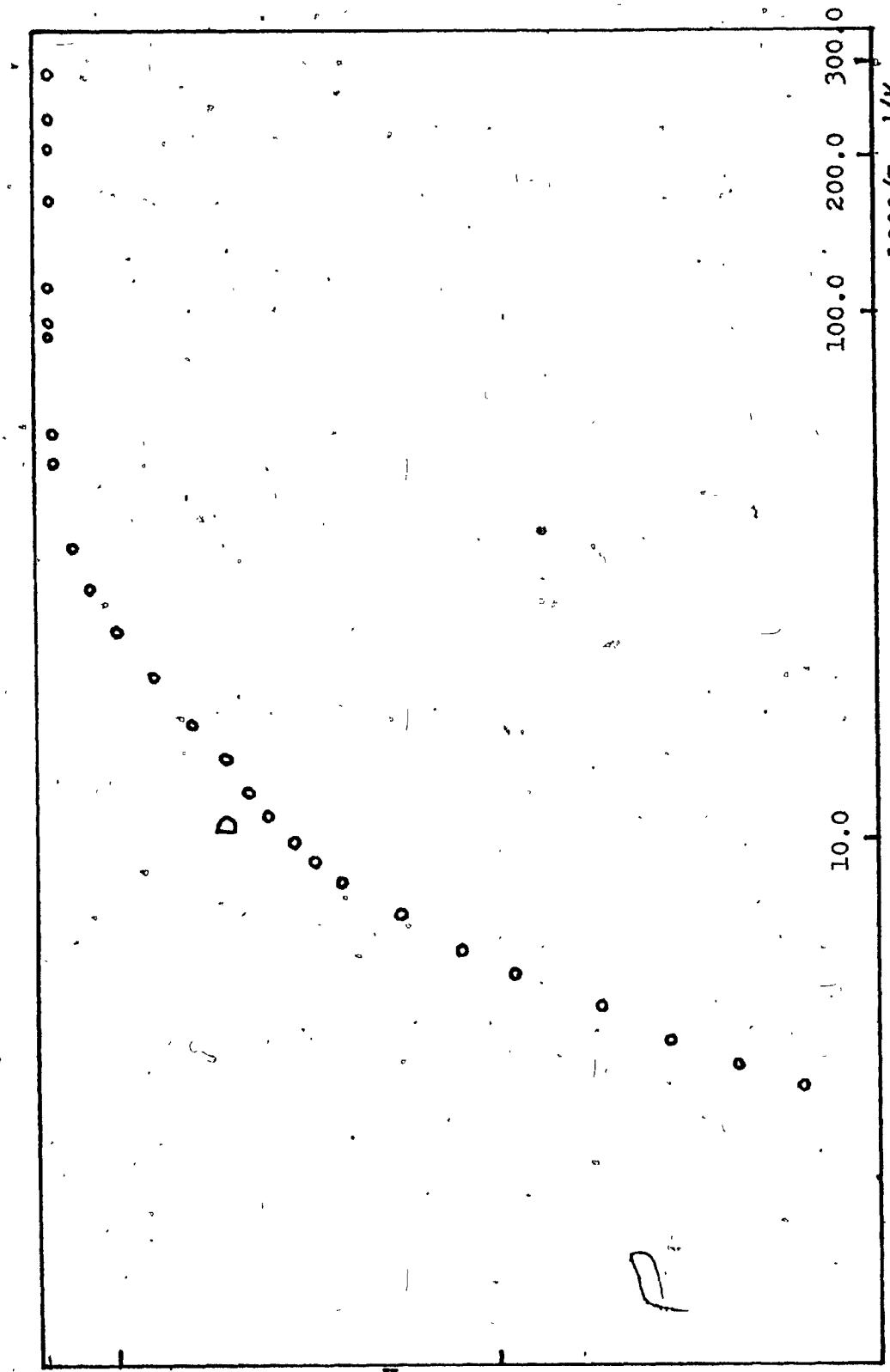

Fig. (5.3) Hall Coefficient as a function of temperature for an annealed sample

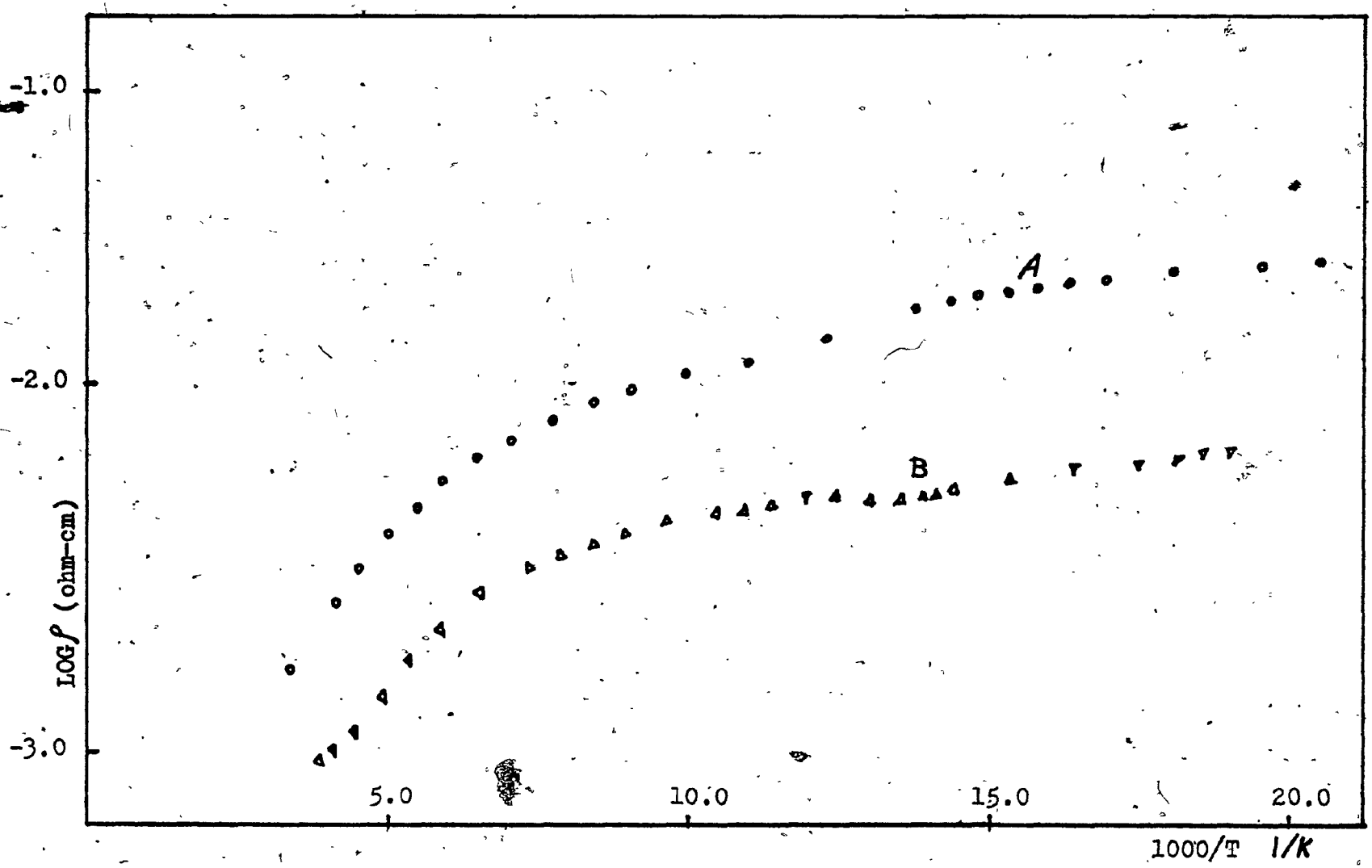

Fig. (5.4) Electrical resistivity as a function of temperature

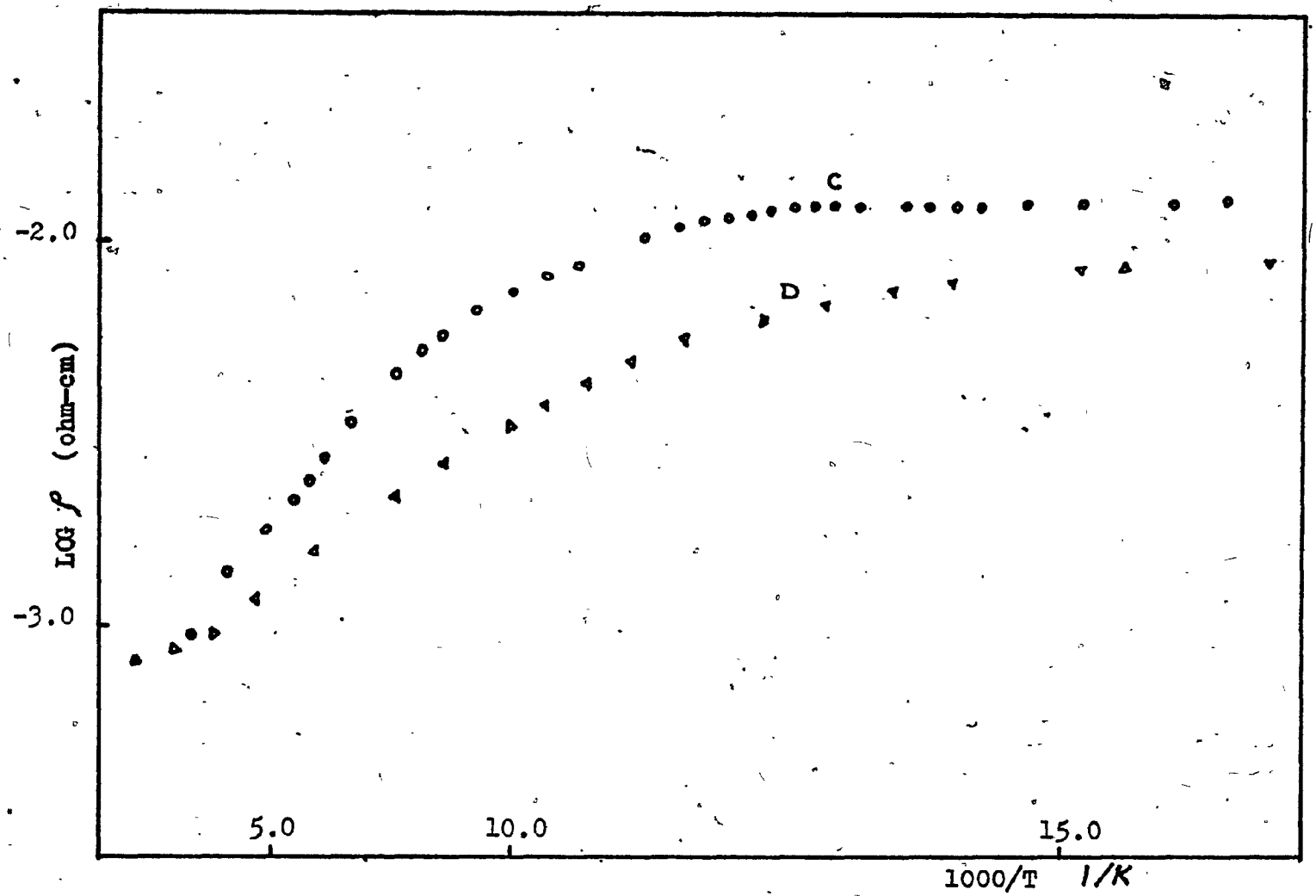

Fig. (5.5) Electrical resistivity as a function of temperature

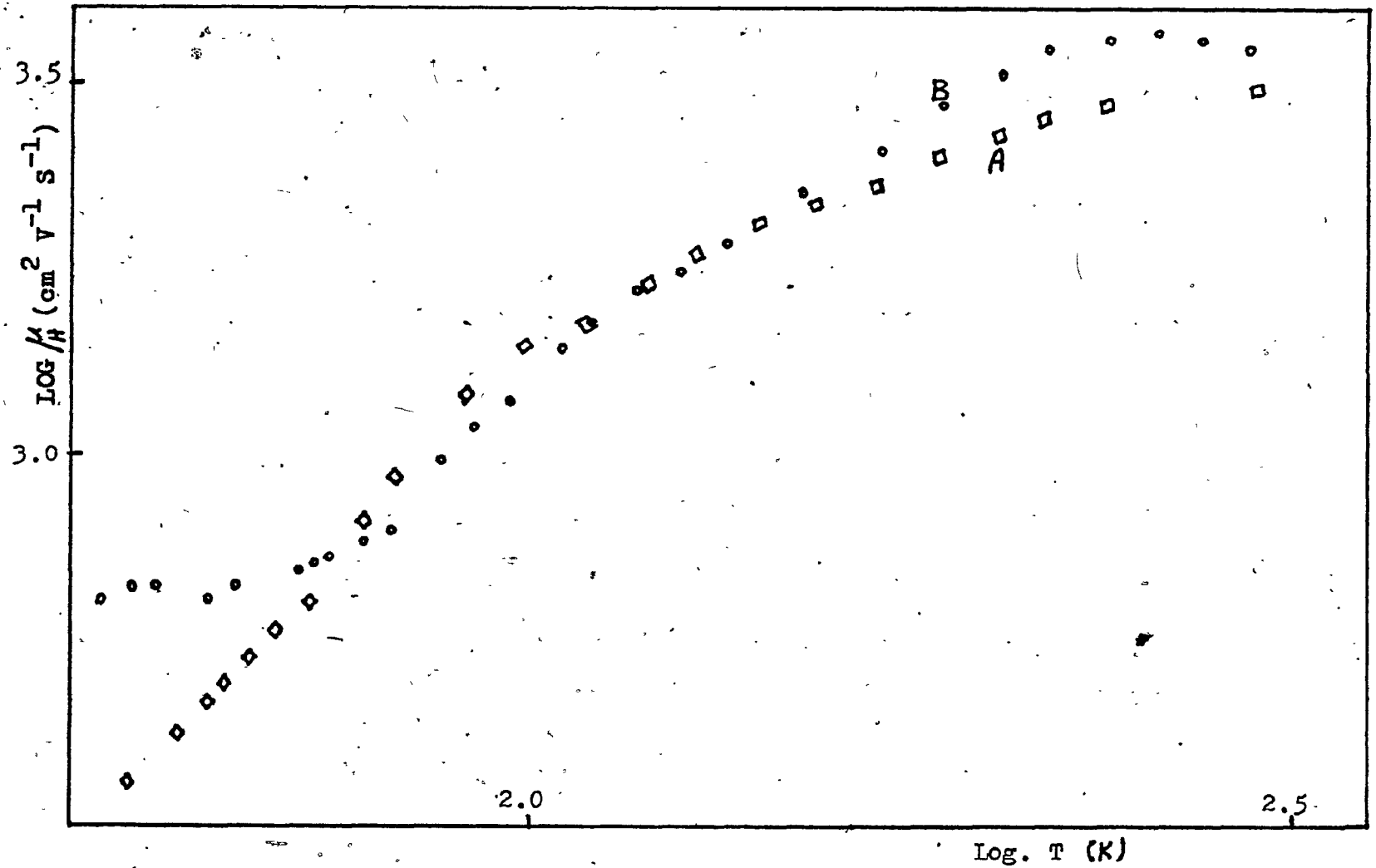

Fig. (5.6) Hall mobility variation versus temperature

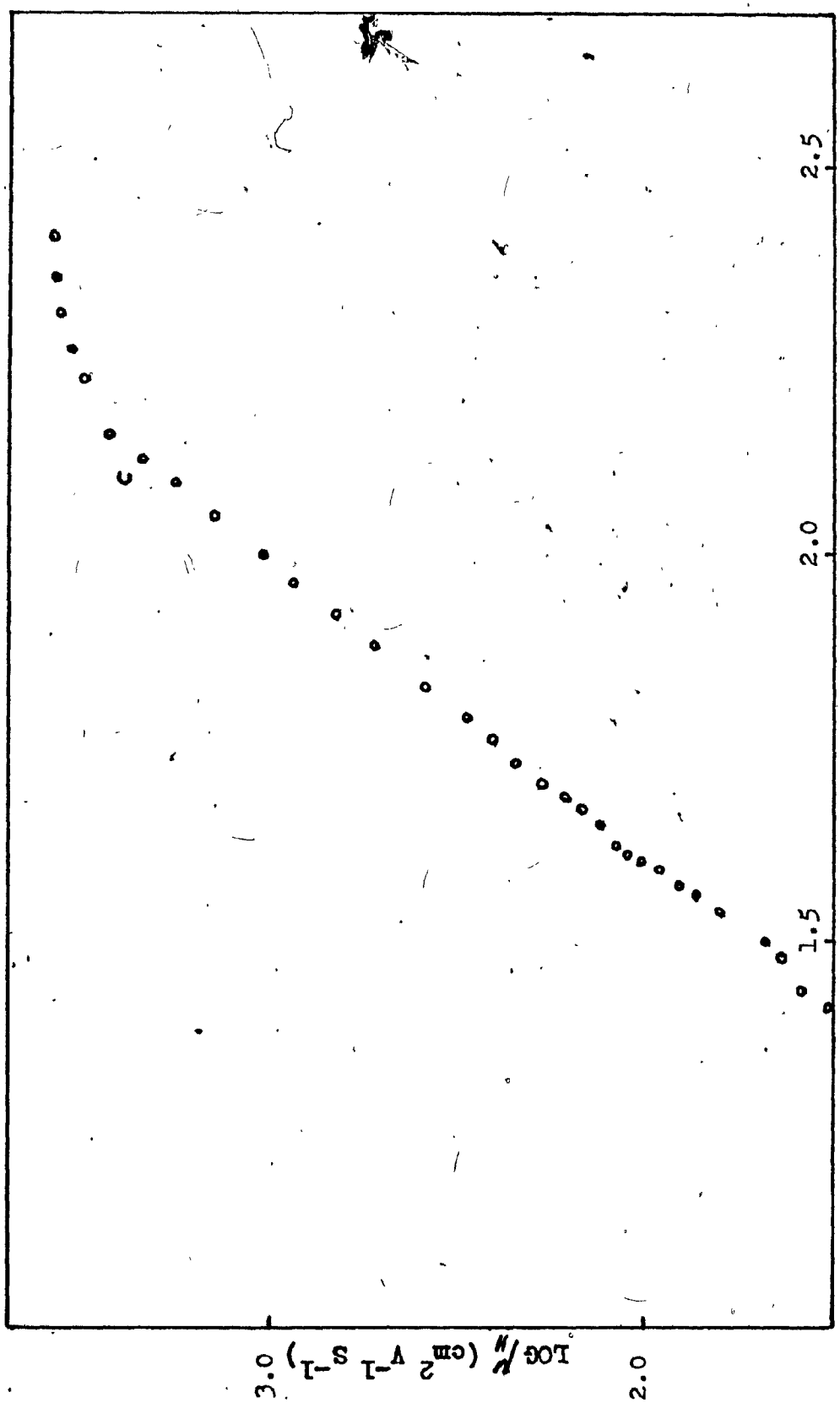

Fig. (5.7) Hall mobility variation versus temperature

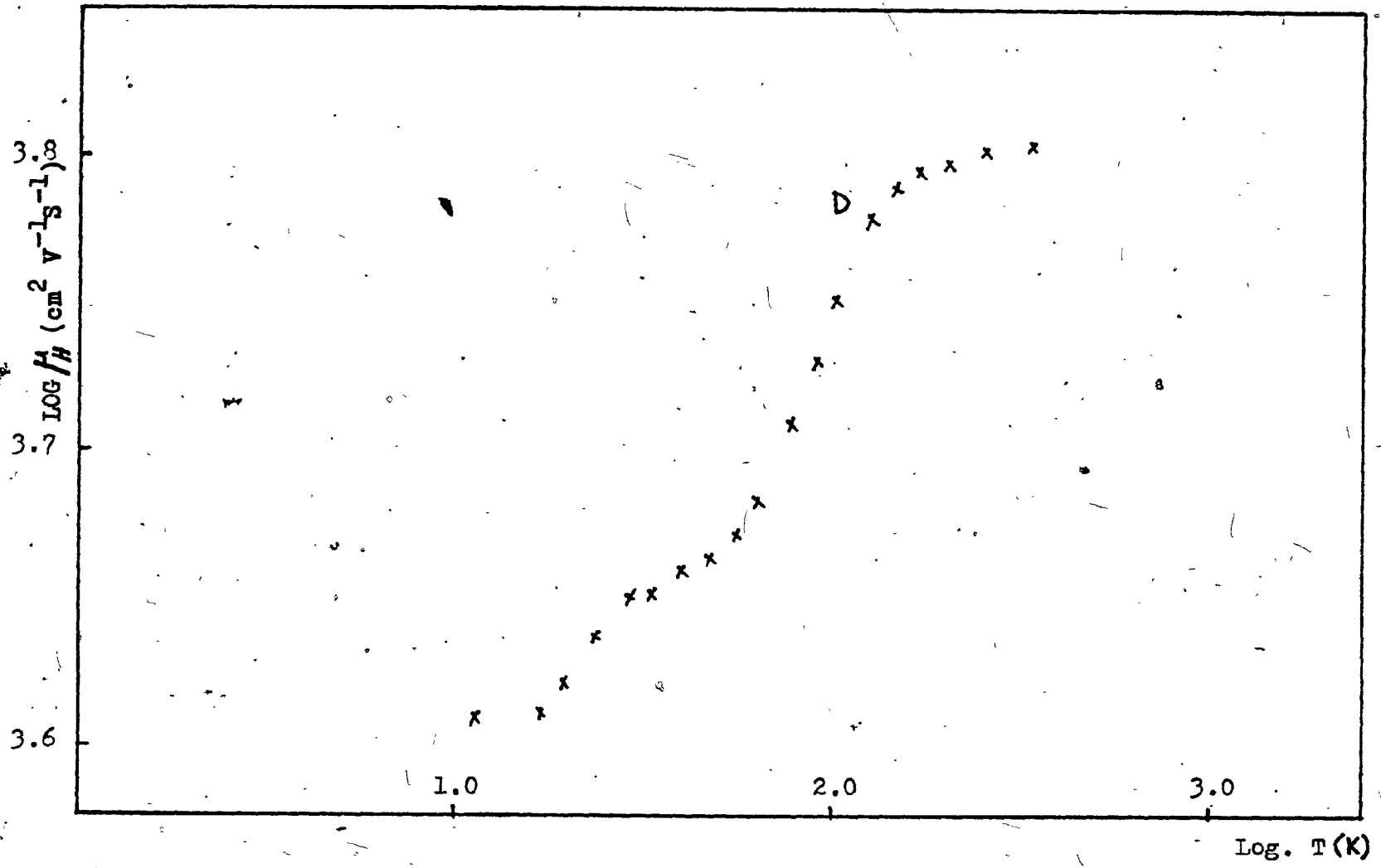

Fig. (5.8) Hall mobility variation of an annealed sample versus temperature

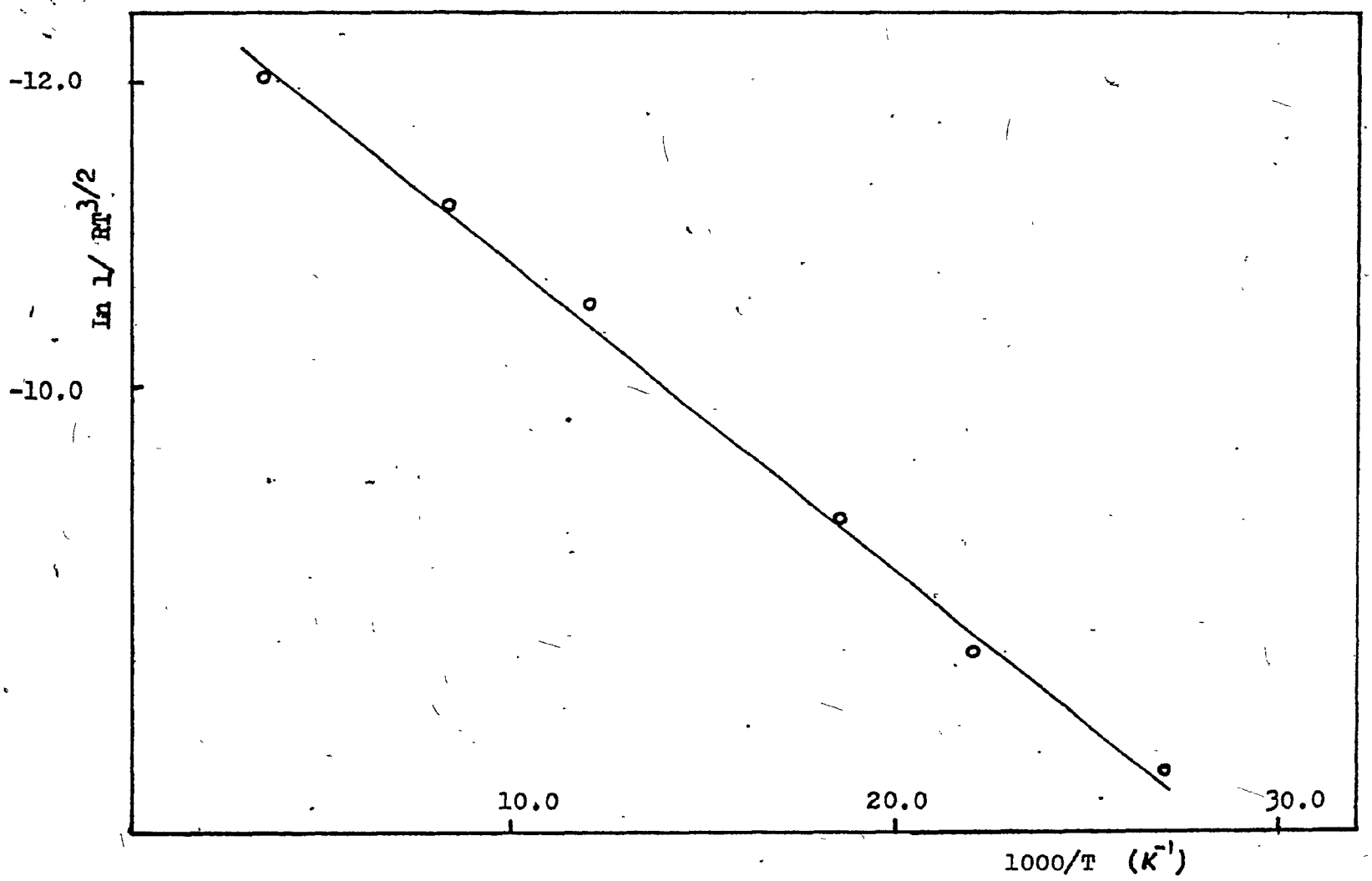

Fig. (5.9) Variation of Ln $1/RT^{3/2}$ versus 1/T

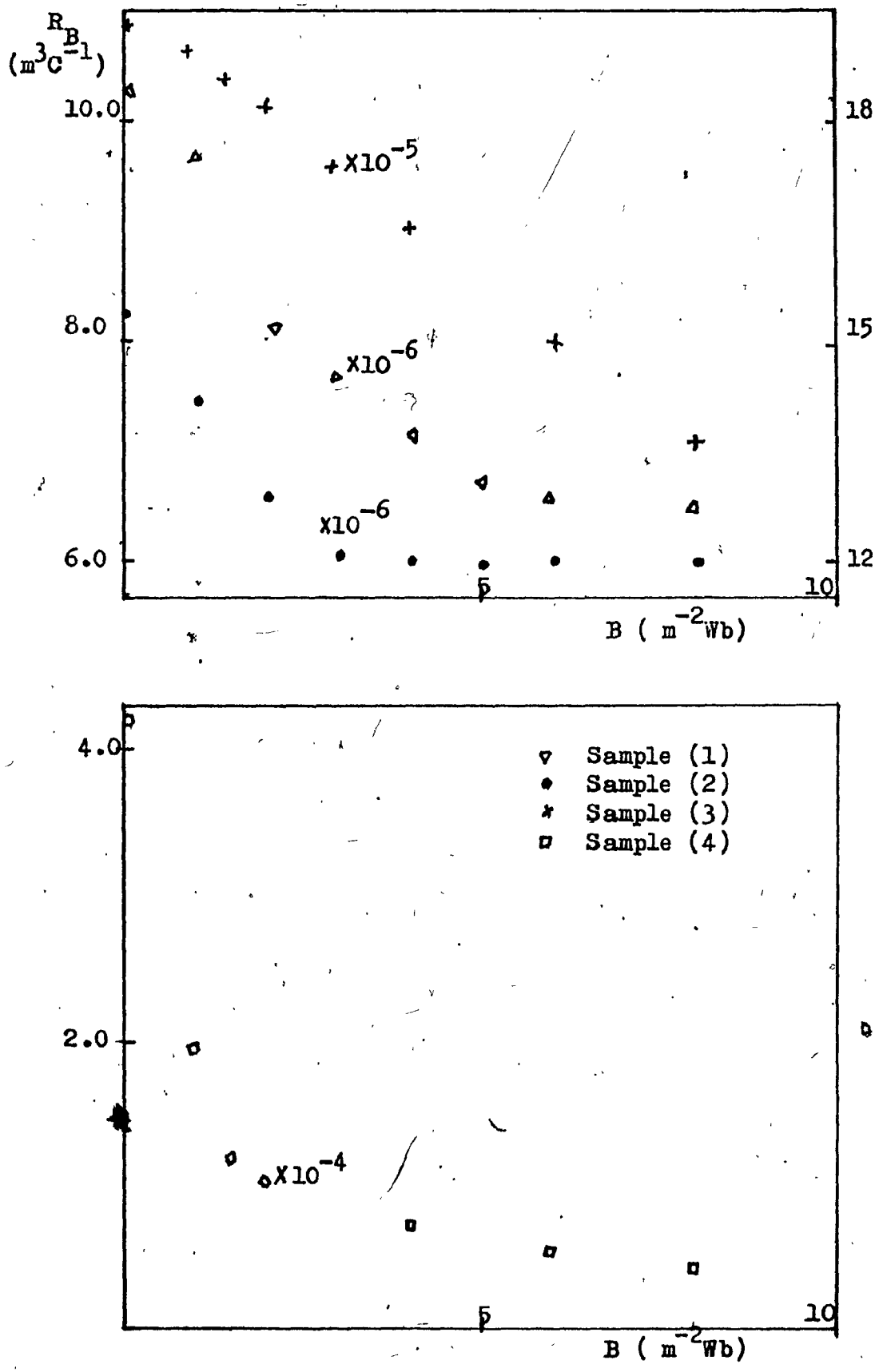

Fig. (5.10) Hall coefficient as a function of magnetic field

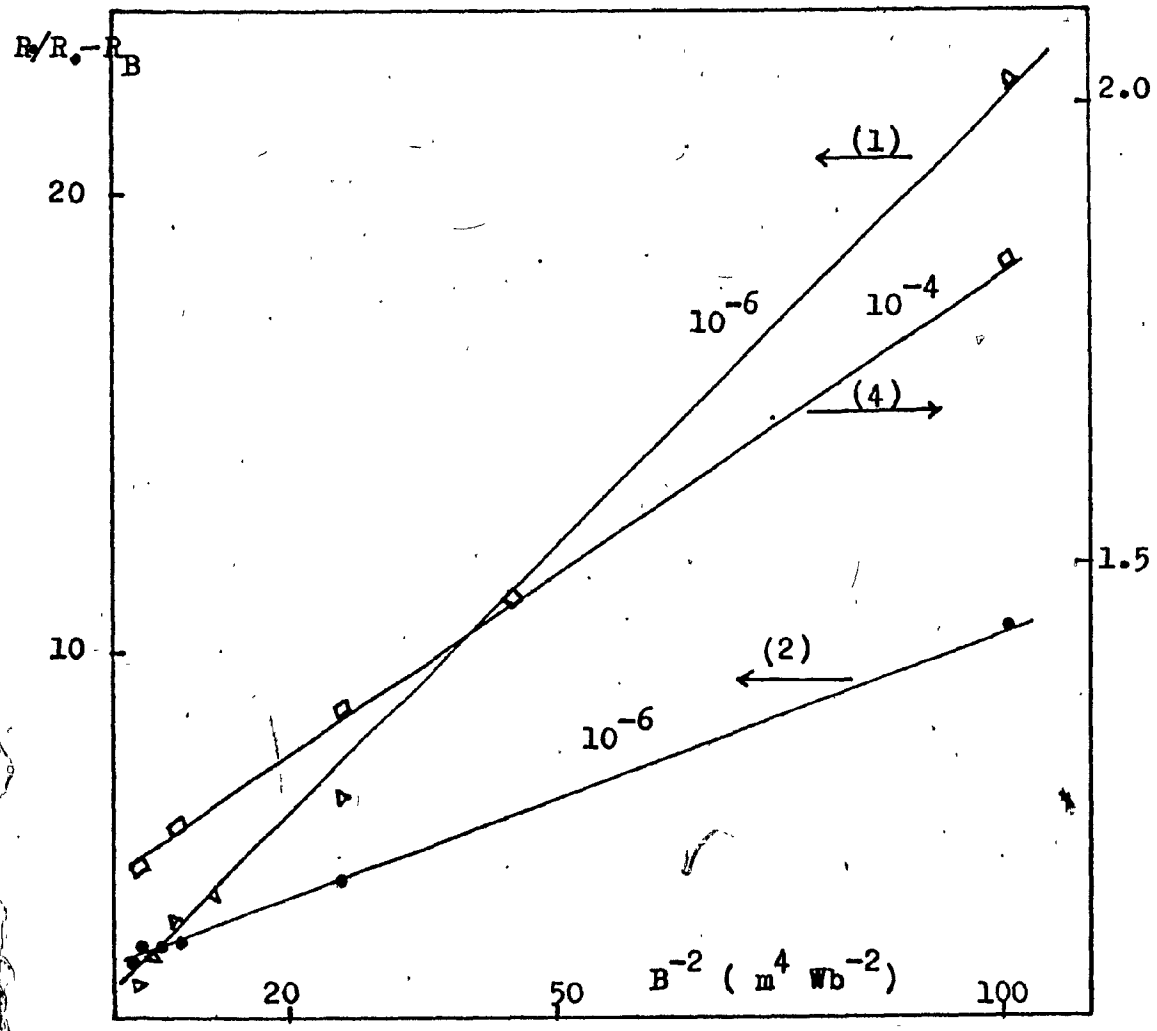

Fig.(5.11) Variation of $R_o/R_o - R_B$ versus B^{-2}

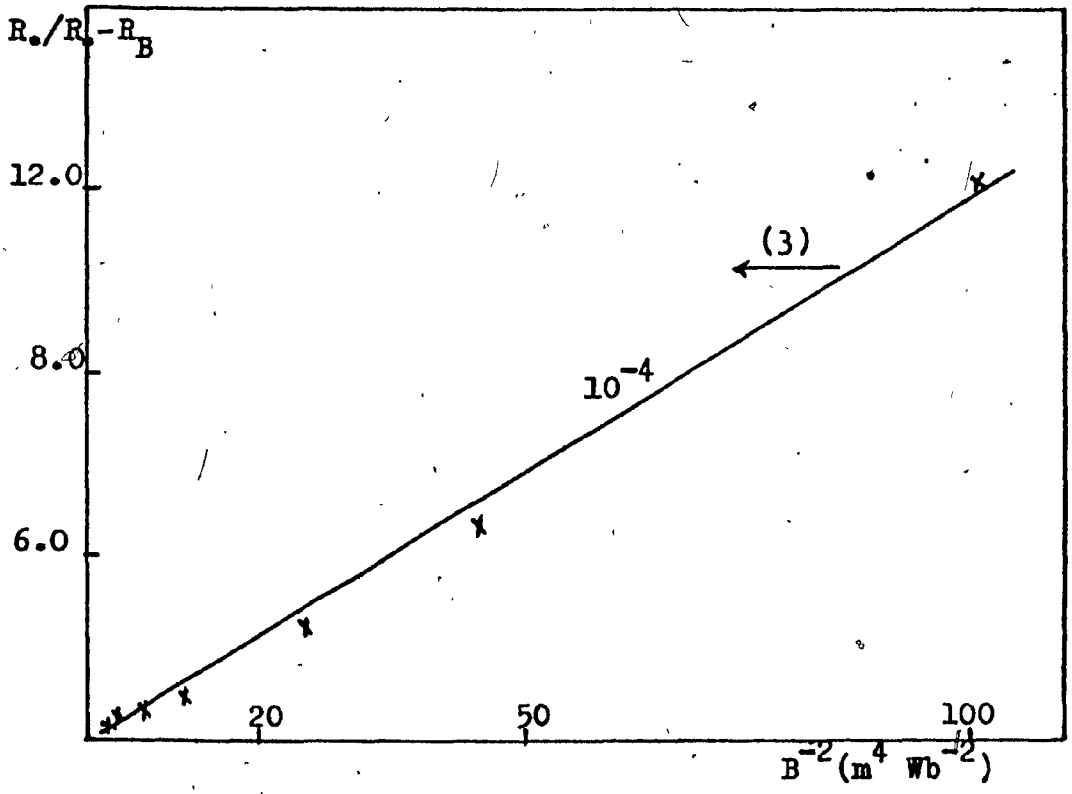

Fig.(5.12) Variation of $R_{\circ}/ R_{\circ}-R_B$ versus B^{-2}

T(K)	22	35	50	75	100	130	180	205	258
$n \times 10^{25}$ (m^{-3})	2.64	.90	.49	.32	.09	.06	.09	.11	.20

Table (5.1) Variation of carrier concentration of sample of HgTe versus temperature

Sample	R_H ($m^3\ C^{-1}$)	σ $(\Omega\ m)^{-1}$	μ_H ($m^2\ V^{-1}\ s^{-1}$)
1	-1.835×10^{-5}	0.77	1.41×10^{-5}
2	-8.2×10^{-6}	1.02	8.36×10^{-6}
3	-1.09×10^{-4}	1.99	2.16×10^{-4}
4	-4.197×10^{-4}	1.99	8.35×10^{-4}

Sample	a	s	n_1 (m^{-3})	n_2 (m^{-3})
			μ_1 ($m^2\ V^{-1}\ s^{-1}$)	μ_2 ($m^2\ V^{-1}\ s^{-1}$)
1	2.47	1.88×10^{-1}	1.8×10^{13}	1.14×10^{24}
			4.2×10^{-1}	4.2×10^{-6}
2	3.20	7.0×10^{-2}	1.26×10^{12}	2.21×10^{24}
			1.99	2.87×10^{-6}
3	2.13	6.06×10^{-1}	4.89×10^{15}	7.77×10^{22}
			1.38×10^{-1}	1.59×10^{-4}
4	1.17	6.41	7.41×10^{13}	1.97×10^{23}
			8.77	6.29×10^{-5}

Table (5.2) Band parameters of different carriers in samples

CHAPTER 6

CONCLUSION

The Hall Coefficient and Electrical resistivity of mercury telluride were measured from 4.2 K to 300 K. The measurements on Hall Coefficient lead us to conclude that the samples are of n - type for the entire temperature range, and the ratio of hole concentration to electron concentration is very small. The results show mercury telluride has a very small energy gap (about 0.01 - 0.03 eV). Low Hall mobility of the samples (in range of $10^{3} cm^{2} V^{-1} S^{-1}$ at room temperature) indicates high vacancy concentration of the HgTe samples, and it is found that the Hall mobility can be improved by annealing the sample.

It is shown that the "Two Band Model" can be used for mercury telluride to characterize different carriers (fast and slow electrons) separately.

REFERENCE

(1) T.C. Harman and A.J. Strauss, J. Appl. Physics suppl. 32, 2265. (1961)

(2) A.J. Strauss, T.C. Harman, D.H. Dickey and M.S. Dresselhaus, Proc. Inc. Conf. Physics of Semiconductors, Exeter, 703 ff. Institute of Physics and the Physical Society, London (1962)

(3) T.C. Harmen, W.H. Kleiner, A.J. Strauss, G.B. Wright, J.G. Marriodes, J.M. Hong and D.H. Dickey, Solid State Commun. 2, 305, (1964)

(4) S. Groves and W. Paul, Phys. Rev. Lett. 11, 194, (1963)

(5) S. Groves and W. Paul, Proc. 7th Inc. Int. Conf., Physics of Semiconductors, p. 41 ff, Dunod, Paris, (1964)

(6) J. Black, S.M. Ku and H.T. Minden, Journal of Electrochemical Society, 105, 723, (1958)

(7) T.C. Harman, M.J. Logan and H.L. Goering, Journal of Physics and Chemistry of Solids, 7, 228, (1958)

(8) W.D. Lawson, S. Nielson, E.H. Putley, and A.S. Young, Journal of Physics and Chemistry of Solids, 9, 325, (1959)

(9) C. Verie and E. Decamps, Physica Status Solidi, 9, 797, (1965)

(10) R. Piotrzkowski, S. Porowski, Z. Dzinba, J. Ginter, W. Girial and L. Sosnowski, Physica Status Solidi, 8, K 135, (1965)

(11) R.A. Stradling, Proceedings of Physical Society, 90, 175, (1967)

(12) T.C. Harman, Physics and Chemistry of II - VI compounds, M. Aven, and J.S. Prener, eds. (North Holland Publishing Co., Amsterdam, 1967) Chapter XV

(13) E.A. Kane, Journal of Physics and Chemistry of Solids, 1, 249, (1957)

(14) N.B. Hanney, Semiconductors, Reinhold Publishing Corporation, New York, (1959)

REFERENCE (con't)

(15) W. Szymanska, Phys. Stat. Sol. 17, 889, (1966)

(16) S.H. Groves, R.N. Brown, C.R. Pidgeon, Interband Magnetoreffection and Band Structure of HgTe Physical Review, 161, 779, (1967)

(17) S.H. Groves, Proceedings of the Conference of Physics of Semimentals and Narrow-Gap Semiconductors. Texas (1970), Carter, D.L., and Bate R.T., eds., (Pergamon Press, New York) 447

(18) R. Piotrzkowski and S. Porowski, II - VI Semiconductors Compounds (Edited by D.G. Thomas) p. 1090. W.A. Benjamin, New York (1967)

(19) E.H. Putley, The Hall Effect and Related Phenomena Butterworths, London, Chapter IV, (1960)

(20) A.C. Beer, suppl. 4, Solid State Physics, F. Seitz and D. Turnbull, eds. (Academic Press, New York, (1963)

(21) ASTM, Standard Method for Measuring Hall Mobility and Hall Coefficient in Extrinsic Semiconductor Single Crystals F 76 - 73.

(22) S. Nielson, Reaction of Indium solder with HgTe, British Journal of Applied Physics, 10, 380, (1959)

(23) R.A. Smith, Semiconductors, Combridge University Press, 187, (1959).

(24) R.G. Chambers, Proc. Phys. Soc. A65, 903, (1952)

(25) C.C.Y, Kwan, J. Basinski, and J.C. Wooley, Phys. Stat. Sol. (b) 48, 699, (1971)

(26) B.A. Lombos, E.Y.M. Lee, A.L. Kipling and R.W. Krawczyniuk, Journal of Physics and Chemistry Solids, 36, 1193 (1975)

(27) L. Sosnowski and R.R. Galazka, Institute of Physics, Polish Academy of Sciences, (II - VI Semiconductors Compounds, by D.G. Thomas) 888, 1967

(28) C. Fau, J. Calas , M. Averous and B.A. Lombos, Can. J. Phys., 56, 610, (1978)

(29) R.O. Carlson, Phys. Rev. 111 , 476 , (1958)

(30) D. LONG, Energy Bands in semiconductors , J. Wiley and sons, Inc. , (1968)